

# Position-Based Transceiver Design for Multiple Satellite to VSAT Downlink

MAIK RÖPER<sup>1</sup>, BHO MATTHIESEN<sup>1,2</sup> (Senior Member, IEEE),  
DIRK WÜBBEN<sup>1</sup> (Senior Member, IEEE), PETAR POPOVSKI<sup>2,3</sup> (Fellow, IEEE),  
AND ARMIN DEKORSY<sup>1</sup> (Senior Member, IEEE)

<sup>1</sup>Gauss-Olbers Center, Department of Communications Engineering, University of Bremen, 28359 Bremen, Germany

<sup>2</sup>U Bremen Excellence Chair, Department of Communications Engineering, University of Bremen, 28359 Bremen, Germany

<sup>3</sup>Department of Electronic Systems, Aalborg University, 9220 Aalborg, Denmark

CORRESPONDING AUTHOR: M. RÖPER (e-mail: roeper@ant.uni-bremen.de)

This work was supported in part by the German Federal Ministry of Education and Research (BMBF) within the project Open6GHub under Grant 16KISK016; in part by the European Space Agency (ESA) under Contract 4000139559/22/UK/AL (AComS); and in part by the German Research Foundation (DFG) under Grant EXC 2077 (University Allowance). This article was presented in part at the 2022 IEEE Wireless Communications and Networking Conference [1] [DOI: 10.1109/WCNC51071.2022.9771777] and at the 2023 IEEE International Conference on Communications [2] [DOI: 10.1109/ICC45041.2023.10279447].

**ABSTRACT** We propose a novel approach for downlink transmission from a satellite swarm towards a very small aperture terminal (VSAT). These swarms have the benefit of much higher spatial separation in the transmit antennas than traditional satellites with antenna arrays, promising a massive increase in spectral efficiency. The resulting precoder and equalizer have only low demands on computational complexity, inter-satellite coordination and channel estimation. This is achieved by taking knowledge about the geometry between satellites and VSAT into account. Due to the position based transceiver design, only slowly changing long-term statistics of the channel coefficient are considered. The necessity of accurate positional information is further relaxed by considering stochastic knowledge about the relative positions between satellites and VSAT rather than exact knowledge. Specifically, each satellite needs only stochastic information about the VSATs' relative positions to calculate its precoding vector. Similarly, the VSAT requires only stochastic knowledge of the satellites' relative positions for equalization. Furthermore, we evaluate the impact the inter-satellite distance has on the achievable data rate. Based on that, an analytic approach to arrange the satellites in a satellite swarm to maximize the rate is provided. The combination of the low complexity transceiver with suitable inter-satellite distances is proven to be capacity achieving in specific scenarios. The simulation results provide evidence that the proposed inter-satellite distance in combination with the proposed transceiver enables close-to-optimal rates in practical applications.

**INDEX TERMS** Small-satellite swarms, distributed precoding, angle division multiple access, 3D networks.

## I. INTRODUCTION

INTEGRATING non-terrestrial networks (NTNs) into terrestrial communication systems is an important step towards truly ubiquitous connectivity [3], [4]. An essential building block is the use of small satellites in low Earth orbit (LEO), currently being deployed by private companies in mega constellations [5], [6], [7]. Compared to traditional high-throughput satellites in medium Earth orbit (MEO) and geostationary orbit (GEO), the main benefits of LEO satellites are much lower propagation delays and deployment costs.

The implementation of multiple-input-multiple-output (MIMO) communication systems has improved the spectral efficiencies in terrestrial networks over the past years [8]. However, in satellite communication, solely increasing the number of transmit and receive antennas per satellite does not necessarily increase the channel capacity [9]. This is due to the fact that satellite communication channel is characterized by a dominant line-of-sight (LoS) connection, leading to correlated channel elements and a rank-deficient channel matrix [10], [11]. In order to increase the spatial diversity, the antennas have to be spatially separated over a large area.

This can be done by utilizing a distributed antenna array either on ground or in the space segment [9], [12]. Indeed, studies have shown that connecting a single ground terminal to multiple satellites increases the channel capacity and the system reliability [13], [14], [15], [16]. Additionally, combining several low cost satellites in swarms leads to increased flexibility and scalability [17]. The geometrical design of these swarms has considerable impact on the communications performance. While swarm layouts with inter-satellite distances ranging from a few meters [18], [19], [20] to several hundreds of kilometer [21], [22] are considered in the literature, the relationship between inter-satellite distance and throughput has not yet been investigated.

Due to the increased spectral efficiency of multi-user systems, downlink precoding has been an active research area during the past decades, both for terrestrial [23], [24], [25] and non-terrestrial communication systems [26], [27], [28]. In particular, the combination of massive MIMO antenna arrays with precoding is a promising approach to boost the system performance for LEO satellite communication [10], [29]. A crucial element for precoding is the availability of accurate channel state information (CSI). Due to the propagation delays and the high relative velocities between LEO satellites and ground terminals, CSI fed back from the ground terminal is already outdated the moment it arrives at the satellites. Therefore, conventional precoding is not suitable for LEO satellite communication. Instead, precoding based on long term statistics and positional information is a promising concept for LEO satellite communications [10], [29], [30], [31]. Compared to full CSI, positional information is easier to obtain and varies significantly slower [32], [33]. Nevertheless, even positional information is usually not perfect. Including the statistics of the estimation error improves the performance of the precoder as well as the equalizer. Such transceivers are commonly called robust transceivers [34].

In terrestrial communication, the design of robust precoders and equalizers that can improve the performance in presence of channel estimation errors is well studied. The most common assumption is that the CSI is perturbed by an additive estimation error [35], [36]. In [37], [38], an extended error model for the precoder design is investigated by taking non-ideal hardware into account, resulting in multiplicative errors which are statistically independent among the antennas. However, such error models are invalid if the transceivers are designed based on positional information. Instead, a multiplicative error model with high correlation among the different antennas is required. In [39], an equalizer is proposed to completely cancel interference from a broader range of possible angles of arrival (AoAs). Another common heuristic approach is given by the so-called diagonal loading method, where a scaled identity matrix is added to the imperfectly estimated autocorrelation matrix in order to increase robustness [40]. Further heuristic robust equalizers are presented in [41], [42], to improve the diagonal loading approach by taking the statistics of

the estimation error into account. In [43], an equalizer to suppress a jamming signal while the desired signal may have its origin in a large geographical region is presented.

In the context of satellite communication, precoding approaches taking imperfect angular information about the ground terminals into account are presented in [44], [45]. In [44], secrecy-energy efficient precoding is considered, whereas the angles of departure (AoDs) of the eavesdroppers are imperfectly known. The AoD uncertainty is modeled as a uniform distribution. In [45], a robust precoder to maximize the sum rate in the downlink (DL) from a single satellite to multiple users on ground is presented. The AoDs to the users are considered to be imperfectly estimated at the satellite, while uniform and Gaussian distributed estimation errors are taken into account. Furthermore, the authors propose to apply supervised learning to approximate the optimal precoder and reduce the numerical complexity. In [46], reinforcement learning is applied to obtain a robust precoder. It is shown that this learned precoder achieves higher sum rates compared to an analytic robust precoder. In particular, reinforcement learning gives significant better results if the receivers are located closely together, while for large distances between the receivers, the sum rates are almost equal. Another approach to deal with imperfect CSI at the transmitter (CSIT) in the downlink is given by rate-splitting multiple access (RSMA) [47], [48]. In satellite communication, RSMA with heuristic precoding can provide higher sum rates compared to spatial division multiple access (SDMA) if the users are located close to each other or if the position error and the transmit power is very large [49]. Since conventional SDMA with low complexity precoding approaches in satellite-to-Earth communication can already achieve very good rates if the users are located far apart, it seems worthwhile to further study the impact of the geometric setup on the achievable rate. While it is not possible to freely chose the position of the ground users in a practical satellite communication scenario, we focus on the DL from a satellite swarm towards a single very small aperture terminal (VSAT) in this paper.

In a satellite swarm, formation flying allows the satellites to orbit the Earth with a constant inter-satellite distance. A popular precoding approach for satellite swarms is the maximum ratio transmission (MRT) [19], [20], [50], [51]. Due to the large virtual antenna array spanned by a satellite swarm, MRT forms very narrow beams, enabling a huge performance gain in terms of signal-to-noise ratio (SNR) [18], [19]. Therefore, satellite swarms are considered a promising approach to directly connects handhelds, which usually have a very low antenna gain, via satellites [19], [20]. However, joint precoding over all satellites within a swarm requires accurate tracking and compensation of the individual propagation delays at the satellites, to ensure that the signals superimpose constructively at the ground terminal [52]. An alternative approach has been presented in [53], where a zero-forcing (ZF) equalizer at the ground terminal is proposed to simultaneously receive transmission from two

satellites. By exploiting the equalization capabilities of a multiple antenna receiver on ground the inter-satellite coordination can be reduced. The authors also numerically evaluate the impact of the inter-satellite distance with respect to (w.r.t.) the outage probability for the signal-to-interference-and-noise ratio (SINR). In this paper, we further analyze, among other things, the impact of the inter-satellite distance on the ergodic rate for an arbitrary number of satellites. We also derive the optimal inter-satellite distance analytically for special cases and show that it serves as a good heuristic in other cases.

The focus of this paper is on the proper design of the distributed precoder and the corresponding equalizer based on stochastic position knowledge as well as the swarm layout. In particular, the main contributions are<sup>1</sup>:

- A low complexity distributed robust precoder for satellite swarms is proposed, where the satellites transmit statistically independent data streams without the need of time critical inter-satellite communication during the transmission. The precoder is derived by considering only imperfect relative positional information of the VSAT w.r.t. the satellites.
- A linear equalizer to maximize the mean SINR at the VSAT is derived based on imperfect relative positional information of the satellites.
- We provide a necessary condition for the satellite swarm layout to be optimal w.r.t. the achievable rate. Furthermore, we propose a closed-form heuristic to obtain a suitable inter-satellite distance and prove its optimality for certain cases.
- Through numerical evaluations, we show that the proposed inter-satellite distance in combination with the proposed transceiver enables close-to-optimal rates. Furthermore, we study the impact of imperfect position knowledge and the non-LoS (NLoS) paths on the achievable rate.

The system model and fundamental results serving as benchmark are introduced in Section II. Then, in Section III, the proposed precoder and equalizer are developed. In Section IV, the optimal distance between the satellites in a swarm is analyzed. This also gives further insight about the optimality of the proposed distributed precoder. Numerical evaluations are provided in Section V, and Section VI concludes the paper.

*Notation:* Column vectors are denoted by bold lowercase letters  $\mathbf{q}$ , while bold uppercase letters denote matrices  $\mathbf{Q}$ . Non-bold symbols denote scalar values  $q$  and  $Q$ . The  $j$ th element of a vector and  $(j, j')$ th elements of a matrix are denoted by  $[\mathbf{q}]_j$  and  $[\mathbf{Q}]_{j,j'}$ , respectively. A set  $\{\mathbf{Q}_1, \dots, \mathbf{Q}_J\}$  is denoted by  $\{\mathbf{Q}_j\}_{j=1}^J$ . Furthermore,  $\text{diag}(q_1, \dots, q_J)$  denotes

a diagonal matrix with elements  $q_1, \dots, q_J$  along its main diagonal. Correspondingly, block diagonal matrices are denoted by  $\text{blkdiag}(\mathbf{Q}_1, \dots, \mathbf{Q}_J)$ . The trace, transpose and conjugate transpose of a matrix  $\mathbf{Q}$  are denoted by  $\text{tr}\{\mathbf{Q}\}$ ,  $\mathbf{Q}^T$  and  $\mathbf{Q}^H$ , respectively. Furthermore,  $|q|$  and  $|\mathbf{Q}|$  are the absolute value of the scalar  $q$  and the determinant of matrix  $\mathbf{Q}$ , respectively. The  $\ell_2$ -norm of a vector  $\mathbf{q}$  is denoted as  $\|\mathbf{q}\|_2$ . Additionally,  $\nabla_{\mathbf{Q}} f(\mathbf{Q}_0)$  denotes the derivative of the function  $f$  w.r.t.  $\mathbf{Q}$  and evaluated at  $\mathbf{Q}_0$ . The expected value is denoted by  $\mathbb{E}\{\cdot\}$ ,  $\mathbf{I}_J$  is the identity matrix of dimension  $J \times J$  and  $\mathbf{0}_{J \times J'}$  is the all zero matrix of dimension  $J \times J'$ . Finally,  $\otimes$  and  $\circ$  denote the Kronecker and Hadamard product of two matrices, respectively.

## II. SYSTEM MODEL AND PERFORMANCE BOUNDS

In this section, we introduce the general system model as well as an upper performance bound to compare the proposed approach with. Due to the movement of satellites, the considered system is time-variant. For the sake of readability, and without loss of generality, we consider only a single time-instance and omit an index to denote that time-instance.

### A. SYSTEM SETUP

Consider a swarm of  $N_S$  satellites which jointly communicate to a common VSAT. The satellites and the VSAT are equipped with planar antenna arrays, building a distributed MIMO system. In particular, for each involved node, i.e., each of the  $N_S$  satellites and the VSAT, define a local coordinate reference system, where the  $xy$ -plane of each local coordinate frame is aligned with the corresponding planar antenna array. This is illustrated in Fig. 1. Thus, the rotation of each node leads to a rotation of the corresponding local coordinate frame. Let  $d_\ell$  be the distance between satellite  $\ell$  and the VSAT. The position of that satellite in the VSAT-centered coordinate system, i.e., the relative position of the satellite w.r.t. the VSAT, is specified by the triplet  $(d_\ell, \theta_\ell^{\text{el}}, \theta_\ell^{\text{az}})$ , where  $\theta_\ell^{\text{el}} \in [0, \pi/2]$  and  $\theta_\ell^{\text{az}} \in [0, 2\pi]$  denote the elevation and azimuth angle in the VSAT-centered coordinate frame, respectively. Equivalently, we can define the satellites position in Cartesian coordinates, where the  $x$ -,  $y$ - and  $z$ -coordinates are

$$d_\ell^x = d_\ell \cos(\theta_\ell^{\text{el}}) \cos(\theta_\ell^{\text{az}}) \quad (1a)$$

$$d_\ell^y = d_\ell \cos(\theta_\ell^{\text{el}}) \sin(\theta_\ell^{\text{az}}) \quad (1b)$$

$$d_\ell^z = d_\ell \sin(\theta_\ell^{\text{el}}), \quad (1c)$$

respectively. Then, we can introduce the space angles

$$\phi_\ell^x = \cos(\theta_\ell^{\text{el}}) \cos(\theta_\ell^{\text{az}}) \quad (2a)$$

$$\phi_\ell^y = \cos(\theta_\ell^{\text{el}}) \sin(\theta_\ell^{\text{az}}) \quad (2b)$$

$$\phi_\ell^z = \sin(\theta_\ell^{\text{el}}). \quad (2c)$$

<sup>1</sup>The proposed distributed precoder and linear equalizer based on perfect position information as well as a preliminary study on the optimal inter-satellite under simplified assumptions have also been presented in [1]. The proposed approach to take statistical knowledge about the receivers position into account for the precoder design has been first presented in [2] for the uplink channel.

With that, the position vector of satellite  $\ell$  in the VSAT-centered coordinate frame is given by

$$\begin{bmatrix} d_\ell^x & d_\ell^y & d_\ell^z \end{bmatrix}^T = d_\ell \cdot \begin{bmatrix} \phi_\ell^x & \phi_\ell^y & \phi_\ell^z \end{bmatrix}^T. \quad (3)$$

For notational brevity, we introduce the variable  $\mathbf{w} \in \{x, y, z\}$  to denote any coordinate axis, e.g., (3) is equivalent to  $d_\ell^w = d_\ell \phi_\ell^w$ .

Note that the position of the satellites is time-variant. In particular, LEO satellites move with very high relative velocities w.r.t. the VSAT. Therefore, we assume that the true position of the satellites at a particular time instance is only *imperfectly* known at the VSAT. Thus, from the VSAT's point of view, the elements of the position vector (3) can be considered as random variables with probability density function (PDF)  $f_{d_\ell^w}(d_\ell^w)$ . Let  $\hat{d}_\ell^w = \mathbb{E}\{d_\ell^w\}$  be the *estimated*  $w$ -coordinate of satellite  $\ell$ , its true position in  $w$  direction can be written as

$$d_\ell^w = \hat{d}_\ell^w + \delta_\ell^w, \quad (4)$$

where  $\delta_\ell^w \in \mathbb{R}$  is the position estimation error in  $w$  direction. Accordingly, we can write the space angle  $\phi_\ell^w$  as

$$\phi_\ell^w = \frac{d_\ell^w}{d_\ell} = \hat{\phi}_\ell^w + \xi_\ell^w \in [-1, 1], \quad (5)$$

where  $\hat{\phi}_\ell^w = \hat{d}_\ell^w/d_\ell$  and  $\xi_\ell^w = \delta_\ell^w/d_\ell$  are the estimated space angle and corresponding estimation error in  $w$  direction, respectively. Let  $f_{\xi_\ell^w}(\xi_\ell^w) \in \mathbb{R}$  be the PDF of the estimation error  $\xi_\ell^w$ , the corresponding characteristic function (CF)  $\varphi_{\xi_\ell^w}(t)$  is defined as [54]

$$\begin{aligned} \varphi_{\xi_\ell^w}(t) &= \mathbb{E}\{\exp(jt\xi_\ell^w)\} \\ &= \int_{-\infty}^{\infty} f_{\xi_\ell^w}(\xi_\ell^w) \cdot \exp(jt\xi_\ell^w) d\xi_\ell^w. \end{aligned} \quad (6)$$

We assume the true position  $d_\ell^w$  to be symmetrically distributed around the estimated position  $\hat{d}_\ell^w$ . Then, the PDF of the estimation error  $\xi_\ell^w$  is symmetric, i.e.,  $f_{\xi_\ell^w}(\xi_\ell^w) = f_{\xi_\ell^w}(-\xi_\ell^w)$ , and its CF is also symmetric and real-valued, i.e.,  $\varphi_{\xi_\ell^w}(t) = \varphi_{\xi_\ell^w}(-t) \in \mathbb{R}$  [54, Th. 8.1]. In Section III-B, the proposed equalizer is derived based on the knowledge of the characteristic function  $\varphi_{\xi_\ell^w}(t)$ . The corresponding precoder at satellite  $\ell$  is based on the statistical knowledge of the VSAT position in the  $\ell$ th satellite-centered coordinate frame, as derived in Section III-A.

Given the triplet  $(d_\ell, \Theta_\ell^{\text{el}}, \Theta_\ell^{\text{az}})$ , as defined in Fig. 1, the Cartesian coordinates of the VSAT in the  $\ell$ th satellite-centered coordinate frame are  $D^{\text{X}\ell} = d_\ell \cos(\Theta_\ell^{\text{el}}) \cos(\Theta_\ell^{\text{az}})$ ,  $D^{\text{Y}\ell} = d_\ell \cos(\Theta_\ell^{\text{el}}) \sin(\Theta_\ell^{\text{az}})$  and  $D^{\text{Z}\ell} = d_\ell \sin(\Theta_\ell^{\text{el}})$ . Accordingly, the corresponding space angles  $\Phi_\ell^{\text{W}\ell} = D^{\text{W}\ell}/d_\ell$ , with  $\text{W}_\ell \in \{\text{X}_\ell, \text{Y}_\ell, \text{Z}_\ell\}$ , are  $\Phi_\ell^{\text{X}\ell} = \cos(\Theta_\ell^{\text{el}}) \cos(\Theta_\ell^{\text{az}})$ ,  $\Phi_\ell^{\text{Y}\ell} = \cos(\Theta_\ell^{\text{el}}) \sin(\Theta_\ell^{\text{az}})$  and  $\Phi_\ell^{\text{Z}\ell} = \sin(\Theta_\ell^{\text{el}})$ . Let  $\hat{\Phi}_\ell^{\text{W}\ell} = \mathbb{E}\{D^{\text{W}\ell}\}/d_\ell$  be the estimated space angle in  $\text{W}_\ell$  direction, we can write

$$\Phi_\ell^{\text{W}\ell} = \hat{\Phi}_\ell^{\text{W}\ell} + \Xi_\ell^{\text{W}\ell} \in [-1, 1], \quad (7)$$

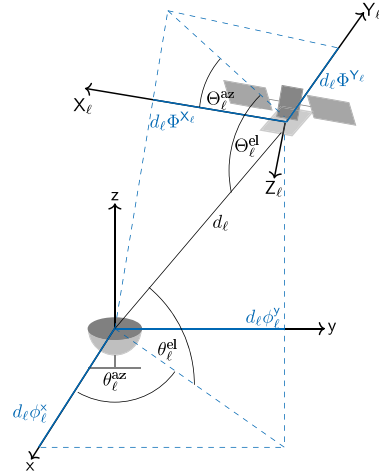


FIGURE 1. Visualization of local coordinate frames.

where  $\Xi_\ell^{\text{W}\ell} \in \mathbb{R}$  is the symmetric estimation error with PDF  $f_{\Xi_\ell^{\text{W}\ell}}(\Xi_\ell^{\text{W}\ell})$ . Thus, its CF is

$$\begin{aligned} \varphi_{\Xi_\ell^{\text{W}\ell}}(t) &= \mathbb{E}\{\exp(jt\Xi_\ell^{\text{W}\ell})\} \\ &= \int_{-\infty}^{\infty} f_{\Xi_\ell^{\text{W}\ell}}(\Xi_\ell^{\text{W}\ell}) \cdot \exp(jt\Xi_\ell^{\text{W}\ell}) d\Xi_\ell^{\text{W}\ell}. \end{aligned} \quad (8)$$

Since the CF is symmetric and real valued, the corresponding PDF is also symmetric and real valued, i.e.,  $f_{\Xi_\ell^{\text{W}\ell}}(\Xi_\ell^{\text{W}\ell}) = f_{\Xi_\ell^{\text{W}\ell}}(-\Xi_\ell^{\text{W}\ell}) \in \mathbb{R} \Leftrightarrow \varphi_{\Xi_\ell^{\text{W}\ell}}(t) = \varphi_{\Xi_\ell^{\text{W}\ell}}(-t) \in \mathbb{R}$ . Furthermore, the position error of the VSAT from the perspective of the  $\ell$ th satellite is  $\Delta^{\text{W}\ell} = d_\ell \Xi_\ell^{\text{W}\ell}$ .

## B. COMMUNICATION MODEL

Satellite  $\ell$  is equipped with an arbitrary planar antenna array consisting of  $N_t$  antennas and the VSAT uses a planar array with  $N_r$  antennas. The satellites jointly transmit a single common message known a priori at all satellites by encoding it in  $M$  independent symbols  $\mathbf{s} \in \mathbb{C}^M$  per time instance using independent and identically distributed (i. i. d.) unit variance Gaussian codebooks. Partitioning the common message into  $M$  data streams requires inter-satellite coordination prior to transmission but no coordination during the transmission. Satellite  $\ell$  employs linear precoding with its local precoding matrix  $\mathbf{G}_\ell \in \mathbb{C}^{N_t \times M}$  to transmit the signal  $\mathbf{x}_\ell = \mathbf{G}_\ell \mathbf{s} \in \mathbb{C}^{N_t}$ . Since all satellites in a swarm are usually of the same type [17], we assume that all satellites have the same average transmit power constraint  $\rho$ , i.e.,  $\text{tr}\{\mathbf{G}_\ell \mathbf{G}_\ell^H\} \leq \rho$  for all  $\ell = 1, \dots, N_S$ . Then, the signal received at the VSAT is

$$\mathbf{y} = \sum_{\ell=1}^{N_S} \mathbf{H}_\ell \mathbf{x}_\ell + \mathbf{n} \quad (9)$$

where  $\mathbf{n}$  is i. i. d. circularly-symmetric complex white Gaussian noise with power  $\sigma_n^2$  and  $\mathbf{H}_\ell \in \mathbb{C}^{N_r \times N_t}$  is the local channel matrix from satellite  $\ell$  to the VSAT.

The satellite-to-ground channel  $\mathbf{H}_\ell$  is typically characterized by a strong LoS path and some nearby reflections on ground, close to the VSAT [31], [55]. The radiated signals

from the individual antennas of satellite  $\ell$  are transmitted over approximately the same distance and are subject to the same atmospheric effects [11]. Therefore, the channels between the different transmit and receive antennas are highly correlated and we can write the channel matrix  $\mathbf{H}_\ell$  from satellite  $\ell$  to the VSAT as

$$\mathbf{H}_\ell = \alpha_\ell \mathbf{a}_\ell \mathbf{b}_\ell^H, \quad (10)$$

where  $\alpha_\ell$  is the i.i.d. complex-valued channel gain from satellite  $\ell$  to the VSAT with  $\mathbb{E}\{\alpha_\ell\} = 0$  and  $\mathbb{E}\{|\alpha_\ell|^2\} = \sigma_{\alpha_\ell}^2$ , and  $\mathbf{a}_\ell$  and  $\mathbf{b}_\ell$  are the array response vectors of the VSAT and satellite  $\ell$ , respectively [31]. The channel gain  $\alpha_\ell$  includes the free space path loss, the atmospheric attenuation, as well as the transmit and receive antenna gain per element, as specified in [55], [56], [57], [58].

Since there are no nearby reflections at the satellites, the transmitted wavefront of satellite  $\ell$  can be well approximated as a plane wave [55]. Therefore, the array response vector  $\mathbf{b}_\ell$  can be written as a steering vector depending on the relative position of the VSAT w.r.t. satellite  $\ell$ , i.e.,  $\mathbf{b}_\ell$  is a function of the space angles  $\Phi^{X_\ell}$  and  $\Phi^{Y_\ell}$ . Let  $(D_{A,n}^{X_\ell}, D_{A,n}^{Y_\ell}, 0)$ , with  $n \in \{1, \dots, N_t\}$ , be the Cartesian coordinates of the  $n$ th antenna of satellite  $\ell$ , given in the  $\ell$ th satellite-centered coordinate frame, the elements of  $\mathbf{b}_\ell$  are given by

$$[\mathbf{b}_\ell]_n = \exp\left(-j\nu\left(D_{A,n}^{X_\ell}\Phi^{X_\ell} + D_{A,n}^{Y_\ell}\Phi^{Y_\ell}\right)\right), \quad (11)$$

where  $\nu$  is the wavenumber of the carrier signal.

The array response vector  $\mathbf{a}_\ell$  on the VSAT side consists of two parts: First, the steering vector  $\mathbf{a}_{\ell,0}$  due to the LoS connection, and secondly, the vector  $\tilde{\mathbf{a}}_\ell$  taking the nearby reflections into account. Let  $\kappa_\ell$  be the Rician factor corresponding to the  $\ell$ th satellite, the array response vector  $\mathbf{a}_\ell$  is given by

$$\mathbf{a}_\ell = \sqrt{\frac{\kappa_\ell}{\kappa_\ell + 1}} \mathbf{a}_{\ell,0} + \sqrt{\frac{1}{\kappa_\ell + 1}} \tilde{\mathbf{a}}_\ell. \quad (12)$$

The elements for the LoS components  $\mathbf{a}_{\ell,0}$  are given by

$$[\mathbf{a}_{\ell,0}]_m = \exp\left(j\nu\left(d_{A,m}^X\phi_\ell^X + d_{A,m}^Y\phi_\ell^Y\right)\right), \quad (13)$$

where  $d_{A,m}^w$  is the distance of the  $m$ th antenna in  $w$  direction from the origin of the VSAT-centered coordinate frame. The vector  $\tilde{\mathbf{a}}_\ell$  is statistically independent of  $\mathbf{a}_{\ell,0}$  and given by the sum of steering vectors from all possible directions from which the reflected waves arrive. Thus its elements can be written as

$$[\tilde{\mathbf{a}}_\ell]_m = \sum_{\ell'=1}^{L_p} \tilde{\alpha}_{\ell,\ell'} \exp\left(j\nu\left(d_{A,m}^X\tilde{\phi}_{\ell,\ell'}^X + d_{A,m}^Y\tilde{\phi}_{\ell,\ell'}^Y\right)\right), \quad (14)$$

where  $L_p$  is the number of possible paths and  $\tilde{\phi}_{\ell,\ell'}^w$  denotes the space angle for the direction of the wave from the  $\ell'$ th path and  $\tilde{\alpha}_{\ell,\ell'}$  is the corresponding i.i.d. complex-valued gain of the  $\ell'$ th path with  $\sum_{\ell'=1}^{L_p} |\tilde{\alpha}_{\ell,\ell'}|^2 = 1$ . Due to the central limit theorem, the NLoS components can be modeled as Gaussian distributed for  $L_p \rightarrow \infty$ . Therefore, we

assume  $\tilde{\mathbf{a}}_\ell \sim \mathcal{CN}(0, \mathbf{R}_{\tilde{\mathbf{a}}_\ell})$  with  $\text{tr}\{\mathbf{R}_{\tilde{\mathbf{a}}_\ell}\} = N_r$ . Substitute (12) into (10), we can write the local channel matrix as

$$\begin{aligned} \mathbf{H}_\ell &= \frac{\alpha_\ell}{\sqrt{\kappa_\ell + 1}} \left( \sqrt{\kappa_\ell} \mathbf{a}_{\ell,0} \mathbf{b}_\ell^H + \tilde{\mathbf{a}}_\ell \mathbf{b}_\ell^H \right) \\ &= \sqrt{\frac{\kappa_\ell}{\kappa_\ell + 1}} \mathbf{H}_{\ell,0} + \sqrt{\frac{1}{\kappa_\ell + 1}} \tilde{\mathbf{H}}_\ell \end{aligned} \quad (15)$$

where  $\mathbf{H}_{\ell,0}$  and  $\tilde{\mathbf{H}}_\ell$  are the channel components for the LoS and NLoS part, respectively.

Note that the space angles involved in (11), (13) and (14) are modeled as random variables due to the imperfect position knowledge. Therefore, the steering vectors  $\mathbf{a}_\ell$  and  $\mathbf{b}_\ell$ , and correspondingly, both channel components  $\mathbf{H}_{\ell,0}$  and  $\tilde{\mathbf{H}}_\ell$  are random variables as well.

### C. UPPER PERFORMANCE BOUND

In the following, an upper bound of the achievable rate is shown based on idealized assumptions. Given perfect synchronization and joint processing among all  $N_S$  satellites within the swarm, the transmission model (9) is equivalent to a point-to-point transmission. In particular, let  $\mathbf{H} = [\mathbf{H}_1 \dots \mathbf{H}_{N_S}]$  be the composite channel matrix and  $\mathbf{x} = [\mathbf{x}_1^T \dots \mathbf{x}_{N_S}^T]^T$  the composite transmit signal. Then, we can write (9) as  $\mathbf{y} = \mathbf{H}\mathbf{x} + \mathbf{n}$ .

Assuming joint precoding over all satellites, the channel capacity for a deterministic channel matrix  $\mathbf{H}$  is [59]

$$\begin{aligned} R_{\text{opt}} &= \max_{\text{tr}\{\mathbf{G}\mathbf{G}^H\} \leq N_S \rho} \log_2 \left| \mathbf{I}_{N_r} + \frac{1}{\sigma_n^2} \mathbf{H}\mathbf{G}\mathbf{G}^H \mathbf{H}^H \right| \\ &= \sum_{\mu=1}^M \log_2 \left( 1 + \lambda_\mu \frac{p_\mu}{\sigma_n^2} \right), \end{aligned} \quad (16)$$

where  $\mathbf{G} = [\mathbf{G}_1^T, \dots, \mathbf{G}_{N_S}^T]^T \in \mathbb{C}^{N_{\text{Tx}} \times M}$  is the joint precoding matrix with  $N_{\text{Tx}} = N_S N_t$  transmit antennas in total and  $\lambda_\mu$  is the  $\mu$ th eigenvalue of  $\mathbf{H}\mathbf{H}^H$ . Note that (16) implies error-free and instantaneous cooperation among the satellites, perfect CSI at the transmitters and receiver, as well as a relaxed sum power constraint. Therefore, this is an upper bound on the capacity of the considered scenario introduced in Section II-B, where imperfect CSI and a per satellite power constraint is assumed.

The optimal precoder in (16) is achieved for

$$\mathbf{G}_{\text{svd}} = \mathbf{V}\mathbf{P}^{\frac{1}{2}}, \quad (17)$$

where the columns of  $\mathbf{V}$  are the  $M = \text{rank}(\mathbf{H}) \leq N_{\text{Tx}}$  right singular vectors of  $\mathbf{H}$ , corresponding to the  $M$  non-zero singular values, and  $\mathbf{P} = \text{diag}(p_1, \dots, p_M)$  is the optimal transmit power allocation obtained from the water-filling algorithm such that  $\sum_{\mu} p_\mu = N_S \rho$ , with  $p_\mu$  being the transmit power of the  $\mu$ th stream [59].

### D. PRACTICAL CONSIDERATIONS

The previously introduced system model includes several common assumptions. In this subsection, we provide a short discussion on the practical feasibility of the main assumptions.

## 1) FEASIBILITY OF OPTIMAL PRECODER

The optimal precoder in (17) is based on a singular value decomposition (SVD) of the global channel matrix  $\mathbf{H}$  which incorporates several assumptions that renders it infeasible for satellite swarms. First of all, an accurate estimate of  $\mathbf{H}$  is required. Due to the fast ground speeds of LEO satellites, the channel coherence time is rather short. Combined with the long round trip times between satellites and VSAT, obtaining this estimate with conventional methods appears to be impossible. Further, assuming a timely and accurate estimate of  $\mathbf{H}_\ell$  exists at satellite  $\ell$ , this estimate would have to be shared with all other satellites within the swarm, leading to additional delay, and thus, ageing of the channel estimate. Finally, the bound in (16) has a relaxed sum power constraint over all satellites that might lead to the violation of the power constraints of individual satellites.

While being of little practical relevance, this optimum joint transmission approach gives the theoretical upper bound for the achievable rate that can serve as benchmark. In Section III, we design a feasible precoder and equalizer that require only knowledge of rather long-term fading statistics and positional knowledge of the VSAT and the satellites, respectively.

## 2) SYNCHRONIZATION

In (9) it is implicitly assumed that a single receiver chain is used at the VSAT. In order to successfully recover the signals from multiple satellites, the sampling clock at the VSAT must be synchronized with every satellite, which can be done with the synchronization signals of 5G [60]. This requires that the signals from all satellites arrive with the same timing and frequency offset at the VSAT. Common state-of-the-art (SotA) precoding approaches for satellite swarms require additional phase alignment for joint beamforming [19], [51], which is usually far more challenging in distributed MIMO settings [61], [62]. Since the proposed precoder in this paper does not require that the satellites form a joint beam, such challenging phase alignment is not required. Therefore, it is sufficient if the satellites ensure that their signals arrive in the same time slots and with the same carrier frequency, i.e., time and frequency synchronization among the satellites must be performed.

Synchronizing the clocks, i.e., frequency synchronization, among the satellites can be done either via a master satellite, which transmits a common reference signal to the satellites, or fully distributed [63]. In any case, inter-satellite communication is required, but the synchronization can be done independently of the VSAT and before the transmission. Therefore, during the transmission, no time-critical inter-satellite communication is required.

Additionally, the transmitted signals are subject to different propagation delays and Doppler shifts. Due to the dominant LoS path, the propagation delay and Doppler shift from satellite  $\ell$  to the VSAT are proportional to the distance  $d_\ell$  and its time derivative  $\dot{d}_\ell$ . Therefore, if the satellites know

their own position and that of the VSAT, they can pre-compensate the delay and Doppler shift. However, for small inter-satellite distances the difference of the propagation delays and Doppler shifts are negligible low. Then, it is sufficient to compensate the mean propagation delay and Doppler shift among the satellites at the VSAT.

Alternatively,  $N_S$  synchronization circuits can be employed at the VSAT to synchronize with each satellite, independently [53], [64]. Then, the satellites don't have to synchronize with each other. However, while multiple synchronization circuits reduce the requirements on inter-satellite coordination, the hardware cost and computational complexity increases. Additionally, the system model has to be slightly modified for multiple synchronization circuits, as shown in Appendix A.

As a side note, the synchronization procedure in the uplink is independently of the number of synchronization circuits at the VSAT. This is because the VSAT can broadcast the synchronization signal to all  $N_S$  satellites in the swarm.

## 3) OBTAINING POSITION INFORMATION

For the proposed transceiver design, the VSAT requires knowledge about the satellites' positions, while the satellites require knowledge about the VSAT's position. In order to obtain the satellites' position at the VSAT, either one of the following three methods is possible:

- The two-line element set (TLE) can be obtained from openly available sources, e.g., provided by [65], [66]. However, this requires an already established connection to the corresponding server.
- The satellites determine their own position, e.g., via global navigation satellite systems (GNSS) sensors, and transmit it down to the VSAT.
- The VSAT estimates the space angles  $\phi_\ell^x$  and  $\phi_\ell^y$ , for all satellites  $\ell$ , from the received signals, e.g., via algorithms proposed in [32], [33].

Likewise, there are three possibilities to obtain the location information from the VSAT at the satellites:

- For static VSAT, the position information of the VSAT can be stored. Then, the satellites can obtain this information from the corresponding data bank.
- The VSAT determines its position via a GNSS and feeds the information to all satellites.
- Satellite  $\ell$  estimates the space angles  $\phi^{X_\ell}$  and  $\phi^{Y_\ell}$  during the uplink, e.g., via algorithms proposed in [32], [33].

Additionally, orbital propagation models can be applied to track and predict the positions [67], [68], without the necessity to constantly receive updates on the positions. Nevertheless, any of the proposed provides only an estimate of the positions for a distinct point in time. Therefore, the obtained position information are usually imperfect.

In Section II-A, we have shown that the error on the space angles  $\Xi_\ell^W$  and  $\xi_\ell^W$  are related to the position errors  $\delta_\ell^W$  and  $\Delta^W_\ell$ , respectively, given by

$$\delta_\ell^W = d_\ell \xi_\ell^W \quad (18a)$$

**TABLE 1.** Impact of rotation  $\tilde{\Theta}$  on position accuracy.

Rotation $\tilde{\Theta}$	Position error $\Delta_\ell^W$	Space angle error $\Xi^{W_\ell}$
$0.1^\circ$	1 km	0.0017
$1^\circ$	10 km	0.017

$$\Delta^{W_\ell} = d_\ell \Xi^{W_\ell}. \quad (18b)$$

In the following, we provide a small toy example to get an intuition about practical position and space angle errors.

Let satellite  $\ell$  be located directly in the zenith of the VSAT, i.e.,  $\theta_\ell^{az} = 0$  and  $\theta_\ell^{el} = \pi/2$ , at an altitude of  $d_0 = d_\ell = 600$  km. The currently available GNSSs allow to determine the own position within few meter radius [69]. To know the position of the VSAT at the satellite and vice versa, the GNSS estimates has to be forwarded over the distance  $d_\ell$ . Given the propagation and processing delay, the GNSS information are available at both nodes after several milliseconds. Since the satellite orbits the Earth with a velocity of  $v \approx 7.56$  km/s = 7.56 m/ms the position uncertainty increases up to some tens of meters. Furthermore, the precoder and equalizer must be kept constant over a certain period of time. This leads to further outdated position information the longer the precoder and equalizer are not updated.

Another important factor which limits the position accuracy are unknown rotations  $\tilde{\Theta}$  of the antenna arrays. For satellites, a Nadir pointing uncertainty  $\tilde{\Theta} \leq 1^\circ$  is possible with common sensors. More advanced technologies enable a Nadir pointing accuracy around  $\tilde{\Theta} \leq 0.1^\circ$  [70], [71]. In Table 1, the corresponding position error  $\Delta^{W_\ell} = d_0 \tan(\tilde{\Theta})$  and the space angle error  $\Xi^{W_\ell} = \sin(\tilde{\Theta})$  are shown for  $\tilde{\Theta} \in \{0.1^\circ, 1^\circ\}$ .

### III. POSITION BASED TRANSCIVER DESIGN

Since the local channel matrix  $\mathbf{H}_\ell$  is described by the outer product of two non-zero vectors (10), its rank is always one, i.e.,  $\text{rank}(\mathbf{H}_\ell) = 1$ . Correspondingly, the global channel matrix  $\mathbf{H} = [\mathbf{H}_1, \dots, \mathbf{H}_{N_S}]$  is given by the concatenation of  $N_S$  rank one matrices and its rank is  $\text{rank}(\mathbf{H}) \leq N_S$ . Given that the steering vectors  $\{\mathbf{a}_i\}_{i=1}^{N_S}$  are linearly independent, the rank of the global channel matrix  $\mathbf{H}$  is  $N_S$ . In practical cases, the steering vectors  $\{\mathbf{a}_i\}_{i=1}^{N_S}$  are always linearly independent because multiple satellites cannot be located at the exact same position. Therefore, we assume  $\text{rank}(\mathbf{H}) = N_S$ .

Furthermore, we define the matrices

$$\mathbf{A} = [\mathbf{a}_1, \dots, \mathbf{a}_{N_S}] \quad (19a)$$

$$\mathbf{B} = \text{blkdiag}(\mathbf{b}_1, \dots, \mathbf{b}_{N_S}). \quad (19b)$$

Note that the columns of the block diagonal matrix  $\mathbf{B}$  are orthogonal and that they are the right singular vectors of  $\mathbf{H}$  corresponding to the non-zero singular values. However, determining the right singular vectors in  $\mathbf{B}$  is only possible if the array response vectors are deterministic. Due to the imperfect position knowledge, this is not the case. Nevertheless, following the derivation from Section II-B, the

capacity can be achieved with  $M = N_S$  independent data streams and it turns out that it is optimal to split these  $N_S$  data streams such that each satellite transmits exactly one of them. In the following, the proposed transceiver is derived under the assumption of imperfect position knowledge as introduced in Section II. First, the precoder is designed to maximize the received signal power. Then, an equalizer is derived to maximize the mean SINR. Finally, in Section III-C, the proposed transceiver for the special case of perfect position knowledge is presented.

#### A. PRECODER DESIGN

Based on the observation that the rank of the channel matrix is  $\text{rank}(\mathbf{H}) = N_S$ , the linear precoder  $\mathbf{G}_{\text{opt}} \in \mathbb{C}^{N_{\text{Tx}} \times N_S}$  is designed to maximize the average received power given the per-satellite power constraint  $\rho$ , i.e., the solution to

$$\begin{aligned} \mathbf{G}_{\text{opt}} \in \arg \max \quad & \mathbb{E} \left\{ \text{tr} \left\{ \mathbf{G}^H \mathbf{H}^H \mathbf{H} \mathbf{G} \right\} \right\} \\ \text{s.t.} \quad & \text{tr} \left\{ \mathbf{G}_\ell^H \mathbf{G}_\ell \right\} \leq \rho, \quad \ell = 1, \dots, N_S. \end{aligned} \quad (20)$$

A solution to (20) is stated in the following proposition.

*Proposition 1:* Let  $\mathbf{g}_{\ell, \text{opt}}$  be a scaled eigenvector corresponding to the largest eigenvalue of  $\mathbf{R}_{\mathbf{b}_\ell} = \mathbb{E} \{ \mathbf{b}_\ell \mathbf{b}_\ell^H \}$ , such that  $\mathbf{g}_{\ell, \text{opt}}^H \mathbf{g}_{\ell, \text{opt}} = \rho$ , for each satellite  $\ell$ . Then an optimal precoder for (20) is

$$\mathbf{G}_{\text{opt}} = \text{blkdiag}(\mathbf{g}_{1, \text{opt}}, \dots, \mathbf{g}_{N_S, \text{opt}}). \quad (21)$$

*Proof:* Due to the statistically independent and zero-mean channel gains  $\{\alpha_i\}_{i=1}^{N_S}$ , we have  $\mathbb{E} \{ \mathbf{H}_\ell^H \mathbf{H}_\ell \} = \mathbf{0}_{N_t \times N_t}$  for all  $i \neq \ell$ . Furthermore, given (10), the local channel correlation matrix is

$$\mathbb{E} \{ \mathbf{H}_\ell^H \mathbf{H}_\ell \} = \sigma_{\alpha_\ell}^2 \mathbb{E} \{ \mathbf{b}_\ell \mathbf{a}_\ell^H \mathbf{a}_\ell \mathbf{b}_\ell^H \} = \sigma_{\alpha_\ell}^2 N_r \mathbf{R}_{\mathbf{b}_\ell}. \quad (22)$$

Thus, the objective function in (20) is equivalent to

$$\mathbb{E} \left\{ \text{tr} \left\{ \mathbf{G}^H \mathbf{H}^H \mathbf{H} \mathbf{G} \right\} \right\} = \text{tr} \left\{ \sum_{\ell=1}^{N_S} \mathbf{G}_\ell^H \mathbb{E} \{ \mathbf{H}_\ell^H \mathbf{H}_\ell \} \mathbf{G}_\ell \right\} \quad (23a)$$

$$= N_r \sum_{\ell=1}^{N_S} \sigma_{\alpha_\ell}^2 \text{tr} \left\{ \mathbf{G}_\ell^H \mathbf{R}_{\mathbf{b}_\ell} \mathbf{G}_\ell \right\}. \quad (23b)$$

Since  $\mathbf{R}_{\mathbf{b}_\ell}$  is positive semi-definite and  $\sigma_{\alpha_\ell}^2$  and  $N_r$  are positive constants, the sum in (23b) is maximized if each term is maximized independently. Thus, the optimization problem (20) is equivalent to

$$\begin{aligned} \forall \ell : \min_{\mathbf{G}_\ell} \quad & -\text{tr} \left\{ \mathbf{G}_\ell^H \mathbf{R}_{\mathbf{b}_\ell} \mathbf{G}_\ell \right\} \\ \text{s.t.} \quad & \text{tr} \left\{ \mathbf{G}_\ell^H \mathbf{G}_\ell \right\} \leq \rho. \end{aligned} \quad (24)$$

The corresponding Lagrangian functions are

$$\begin{aligned} \mathcal{L}_{\text{PC}}(\mathbf{G}_\ell, \omega_\ell) = \quad & -\text{tr} \left\{ \mathbf{G}_\ell^H \mathbf{R}_{\mathbf{b}_\ell} \mathbf{G}_\ell \right\} \\ & + \omega_\ell \left( \text{tr} \left\{ \mathbf{G}_\ell^H \mathbf{G}_\ell \right\} - \rho \right), \end{aligned} \quad (25)$$

where  $\omega_\ell \geq 0$  is the Lagrange multiplier corresponding to the  $\ell$ th satellite power constraint.

We leverage [72, Proposition 3.3.4] to find the solution of (24). Every stationary point  $\mathbf{G}'_\ell$  satisfies  $\nabla_{\mathbf{G}} \mathcal{L}_{\text{PC}}(\mathbf{G}'_\ell, \omega'_\ell) = -\mathbf{G}'_\ell{}^H \mathbf{R}_{\mathbf{b}_\ell} + \omega'_\ell \mathbf{G}'_\ell{}^H = \mathbf{0}$ , for some  $\omega'_\ell$ . This is equivalent to

$$\mathbf{R}_{\mathbf{b}_\ell} \mathbf{G}'_\ell = \omega'_\ell \mathbf{G}'_\ell. \quad (26)$$

Then, substituting (26) into (25), the Lagrangian at the stationary point  $(\mathbf{G}'_\ell, \omega'_\ell)$  evaluates to

$$\begin{aligned} \mathcal{L}_{\text{PC}}(\mathbf{G}'_\ell, \omega'_\ell) &= -\text{tr}\left\{\mathbf{G}'_\ell{}^H \mathbf{R}_{\mathbf{b}_\ell} \mathbf{G}'_\ell\right\} \\ &= -\omega'_\ell \text{tr}\left\{\mathbf{G}'_\ell{}^H \mathbf{G}'_\ell\right\} \geq -\omega'_{\ell, \max} \rho, \end{aligned} \quad (27)$$

where  $\omega'_{\ell, \max}$  is the maximum eigenvalue of  $\mathbf{R}_{\mathbf{b}_\ell}$ . Given the proposed precoder  $\mathbf{G}_{\ell, \text{opt}} = [\mathbf{0}_{N_t \times (\ell-1)}, \mathbf{g}_{\ell, \text{opt}}, \mathbf{0}_{N_t \times (N_s - \ell)}]$ , equality in (27) holds. Correspondingly, the Lagrangian (25) is minimized and a global optimum for (20) is achieved. ■

A direct consequence of the block diagonal precoding matrix  $\mathbf{G}_{\text{opt}}$  is that each satellite transmits a different independent stream  $s_\ell$  of the whole data vector  $\mathbf{s}$ , i.e., the transmit signal of satellite  $\ell$  is  $\mathbf{x}_\ell = \mathbf{G}_{\ell, \text{opt}} \mathbf{s} = \mathbf{g}_{\ell, \text{opt}} s_\ell$ . Furthermore, the precoding vector  $\mathbf{g}_{\ell, \text{opt}}$  for satellite  $\ell$  is independent of the precoding vectors  $\mathbf{g}_{i, \text{opt}}$  for the other satellites  $i \neq \ell$ . Instead, satellite  $\ell$  only has to know the statistics of its space angles  $\Phi^{X_\ell}$  and  $\Phi^{Y_\ell}$ . This implies that the optimal solution for (20) can be obtained if the data stream is split among the satellites and each satellite calculates its precoding vector locally.

*Remark 1:* The precoder  $\mathbf{G}_{\text{opt}}$  in Proposition 1 is optimal in the sense that the signal power is maximized at the receiver. This does not imply that  $\mathbf{G}_{\text{opt}}$  is optimal w.r.t. the achievable rate, i.e.,  $\mathbf{G}_{\text{opt}} \neq \mathbf{G}_{\text{svd}}$ , in general. In Section IV, it is shown under which condition  $\mathbf{G}_{\text{opt}}$  maximizes the achievable rate, too.

The solution in Proposition 1 requires an eigendecomposition of the autocorrelation matrix of the steering vectors  $\mathbf{R}_{\mathbf{b}_\ell} = \mathbb{E}\{\mathbf{b}_\ell \mathbf{b}_\ell^H\}$ . From the CFs  $\varphi_{\Xi^{X_\ell}}(t)$  and  $\varphi_{\Xi^{Y_\ell}}(t)$  of the estimation errors  $\Xi^{X_\ell}$  and  $\Xi^{Y_\ell}$ , respectively, as defined in (8), the  $(n, n')$ th element of the autocorrelation matrix  $\mathbf{R}_{\mathbf{b}_\ell}$  is obtained as

$$\begin{aligned} [\mathbf{R}_{\mathbf{b}_\ell}]_{n, n'} &= \mathbb{E}\left\{\exp\left(-j\nu\left(D_{A, n}^{X_\ell} \Phi^{X_\ell} + D_{A, n}^{Y_\ell} \Phi^{Y_\ell} - D_{A, n'}^{X_\ell} \Phi^{X_\ell} - D_{A, n'}^{Y_\ell} \Phi^{Y_\ell}\right)\right)\right\} \\ &= \exp\left(-j\nu\left(\left(D_{A, n}^{X_\ell} - D_{A, n'}^{X_\ell}\right) \hat{\Phi}^{X_\ell} + \left(D_{A, n}^{Y_\ell} - D_{A, n'}^{Y_\ell}\right) \hat{\Phi}^{Y_\ell}\right)\right) \\ &\quad \cdot \varphi_{\Xi^{X_\ell}}\left(\nu\left(D_{A, n}^{X_\ell} - D_{A, n'}^{X_\ell}\right)\right) \\ &\quad \cdot \varphi_{\Xi^{Y_\ell}}\left(\nu\left(D_{A, n}^{Y_\ell} - D_{A, n'}^{Y_\ell}\right)\right). \end{aligned} \quad (28)$$

The eigendecomposition has to be performed every time an estimated space angle  $\hat{\Phi}^{X_\ell}$  or  $\hat{\Phi}^{Y_\ell}$  or the statistics of the estimation errors  $\Xi^{X_\ell}$  or  $\Xi^{Y_\ell}$  changes. Given the special

structure of the autocorrelation matrix  $\mathbf{R}_{\mathbf{b}_\ell}$ , the computational complexity of the optimal precoder  $\mathbf{g}_{\ell, \text{opt}}$  can be reduced for slowly changing statistics of the estimation errors  $\Xi^{X_\ell}$  or  $\Xi^{Y_\ell}$ . For that, let  $\mathbf{R}_{\varphi_{\Xi}}$  be the correlation matrix of the estimation error and  $\hat{\mathbf{b}}_\ell$  the estimated array response vector at satellite  $\ell$  with elements

$$[\mathbf{R}_{\varphi_{\Xi}}]_{n, n'} = \varphi_{\Xi^{X_\ell}}\left(\nu\left(D_{A, n}^{X_\ell} - D_{A, n'}^{X_\ell}\right)\right) \cdot \varphi_{\Xi^{Y_\ell}}\left(\nu\left(D_{A, n}^{Y_\ell} - D_{A, n'}^{Y_\ell}\right)\right) \quad (29)$$

$$[\hat{\mathbf{b}}_\ell]_n = \exp\left(-j\nu\left(D_{A, n}^{X_\ell} \hat{\Phi}^{X_\ell} + D_{A, n}^{Y_\ell} \hat{\Phi}^{Y_\ell}\right)\right), \quad (30)$$

respectively. Then, the optimal precoder (21) can be obtained by weighting the elements of the estimated steering vector  $\hat{\mathbf{b}}_\ell$ , as stated in the following proposition.

*Proposition 2:* Let  $\mathbf{w}$  be the eigenvector corresponding to the largest eigenvalue of  $\mathbf{R}_{\varphi_{\Xi}}$ . Then, the optimal precoding vector  $\mathbf{g}_{\ell, \text{opt}}$  is

$$\mathbf{g}_{\ell, \text{opt}} = \sqrt{\frac{\rho}{N_t}} \hat{\mathbf{b}}_\ell \circ \mathbf{w}, \quad (31)$$

where  $\circ$  denotes the Hadamard product, i.e., element-wise multiplication of the vector elements.

*Proof:* Let  $\mathbf{D}_{\hat{\mathbf{b}}_\ell} = \text{diag}\left([\hat{\mathbf{b}}_\ell]_1, \dots, [\hat{\mathbf{b}}_\ell]_{N_s}\right)$ . Then, the autocorrelation matrix  $\mathbf{R}_{\mathbf{b}_\ell}$  can be decomposed as

$$\mathbf{R}_{\mathbf{b}_\ell} = \mathbf{D}_{\hat{\mathbf{b}}_\ell} \mathbf{R}_{\varphi_{\Xi}} \mathbf{D}_{\hat{\mathbf{b}}_\ell}^H. \quad (32)$$

Since  $\mathbf{g}_{\ell, \text{opt}}/\sqrt{\rho}$  is the eigenvector corresponding to the largest eigenvalue  $\lambda_{\max}$  of  $\mathbf{R}_{\mathbf{b}_\ell}$ , we have

$$\mathbf{D}_{\hat{\mathbf{b}}_\ell} \mathbf{R}_{\varphi_{\Xi}} \mathbf{D}_{\hat{\mathbf{b}}_\ell}^H \mathbf{g}_{\ell, \text{opt}} = \lambda_{\max} \mathbf{g}_{\ell, \text{opt}} \quad (33a)$$

$$\Leftrightarrow \mathbf{R}_{\varphi_{\Xi}} \mathbf{D}_{\hat{\mathbf{b}}_\ell}^H \mathbf{g}_{\ell, \text{opt}} = \lambda_{\max} \mathbf{D}_{\hat{\mathbf{b}}_\ell}^H \mathbf{g}_{\ell, \text{opt}} \quad (33b)$$

Since (31) is equivalent to

$$\mathbf{g}_{\ell, \text{opt}} = \sqrt{\frac{\rho}{N_t}} \mathbf{D}_{\hat{\mathbf{b}}_\ell} \mathbf{w}, \quad (34)$$

it is a solution to (33b), which can be verified by plugging (34) into (33b), i.e.,

$$\mathbf{R}_{\varphi_{\Xi}} \mathbf{D}_{\hat{\mathbf{b}}_\ell}^H \sqrt{\frac{\rho}{N_t}} \mathbf{D}_{\hat{\mathbf{b}}_\ell} \mathbf{w} = \lambda_{\max} \mathbf{D}_{\hat{\mathbf{b}}_\ell}^H \sqrt{\frac{\rho}{N_t}} \mathbf{D}_{\hat{\mathbf{b}}_\ell} \mathbf{w} \quad (35a)$$

$$\Leftrightarrow \mathbf{R}_{\varphi_{\Xi}} \mathbf{w} = \lambda_{\max} \mathbf{w}. \quad (35b)$$

■

With Proposition 2, an eigendecomposition is only required if the statistics of the phase errors  $\Xi_\ell^w$  changes. As long as these statistics do not change, the optimal precoding vector  $\mathbf{g}_{\ell, \text{opt}}$  can be obtained by simply weighting the elements of the estimated steering vector  $\hat{\mathbf{b}}_\ell$ .

## B. LINEAR EQUALIZATION AT GROUND STATION

In the previous subsection, it was shown that an optimal precoder can be obtained if each satellite transmits a data stream independently of the other satellites in the swarm. Therefore, we assume in the following any block diagonal precoding matrix  $\mathbf{G} = \text{blkdiag}(\mathbf{g}_1, \dots, \mathbf{g}_{N_s})$  with  $\mathbf{g}_\ell \in \mathbb{C}^{N_t}$ .

This enables linear equalization at the VSAT based on the satellites position to recover the  $N_S$  data streams, as shown in the following.

After linear equalization with  $\mathbf{W} = [\mathbf{w}_1, \dots, \mathbf{w}_{N_S}]^H \in \mathbb{C}^{N_S \times N_r}$ , the  $\ell$ th estimated stream is

$$\begin{aligned} \hat{s}_\ell &= \mathbf{w}_\ell^H \mathbf{y} \\ &= \mathbf{w}_\ell^H \mathbf{H}_\ell \mathbf{g}_\ell s_\ell + \mathbf{w}_\ell^H \left( \sum_{i \neq \ell} \mathbf{H}_i \mathbf{g}_i s_i + \mathbf{n} \right). \end{aligned} \quad (36)$$

Assuming the use of capacity achieving point-to-point codes for each stream, the achievable rate  $R_{\text{lin}}$  is the sum over the maximum per-stream rates [8, Sec. 8.3], i.e.,

$$R_{\text{lin}} = \sum_{\ell=1}^{N_S} R_\ell = \sum_{\ell=1}^{N_S} \log_2(1 + \Gamma_\ell) \quad (37)$$

where

$$\Gamma_\ell = \frac{|\mathbf{w}_\ell^H \mathbf{H}_\ell \mathbf{g}_\ell|^2}{\sum_{i \neq \ell} |\mathbf{w}_\ell^H \mathbf{H}_i \mathbf{g}_i|^2 + \sigma_n^2 \mathbf{w}_\ell^H \mathbf{w}_\ell} \quad (38)$$

is the effective SINR of the  $\ell$ th stream. Observe that  $\Gamma_\ell$  is not a function of  $\mathbf{w}_i$  for  $i \neq \ell$ . Thus, the rate in (37) is maximized by maximizing each term separately. Due to the monotonicity of the logarithm, this optimum is attained at the maximum  $\Gamma_\ell$ .

However, the instantaneous SINR in (38) depends on the actual channel realization  $\mathbf{H}$ . Given the assumptions from Section II, only statistical information about  $\mathbf{H}$  is available at the VSAT. Therefore, we optimize the ergodic SINR instead of the instantaneous, i.e.,

$$\mathbf{w}_{\ell, \text{opt}} \in \arg \max_{\mathbf{w}_\ell} \mathbb{E} \left\{ \frac{|\mathbf{w}_\ell^H \mathbf{H}_\ell \mathbf{g}_\ell|^2}{\sum_{i \neq \ell} |\mathbf{w}_\ell^H \mathbf{H}_i \mathbf{g}_i|^2 + \sigma_n^2 \mathbf{w}_\ell^H \mathbf{w}_\ell} \right\}. \quad (39)$$

Solving (39) requires to evaluate the channel correlation matrix  $\mathbb{E}\{\mathbf{H}_\ell \mathbf{H}_\ell^H\}$ . Given the channel model (15), it is given by

$$\begin{aligned} \mathbb{E}\{\mathbf{H}_\ell \mathbf{H}_\ell^H\} &= \frac{\sigma_{\alpha_\ell}^2}{\kappa_\ell + 1} \left( \mathbb{E}\{\kappa_\ell \mathbf{a}_{\ell,0} \mathbf{b}_\ell^H \mathbf{b}_\ell \mathbf{a}_{\ell,0}^H\} \right. \\ &\quad \left. + \mathbb{E}\{\tilde{\mathbf{a}}_\ell \mathbf{b}_\ell^H \mathbf{b}_\ell \tilde{\mathbf{a}}_\ell^H\} \right) \\ &= \frac{\sigma_{\alpha_\ell}^2 N_t}{\kappa_\ell + 1} (\kappa_\ell \mathbf{R}_{\mathbf{a}_{\ell,0}} + \mathbf{R}_{\tilde{\mathbf{a}}_\ell}), \end{aligned} \quad (40)$$

where  $\mathbf{R}_{\mathbf{a}_{\ell,0}}$  and  $\mathbf{R}_{\tilde{\mathbf{a}}_\ell}$  are the autocorrelation matrices of the steering vector  $\mathbf{a}_\ell$  corresponding to the LoS and NLoS paths, respectively.

Given the CFs of the  $\ell$ th satellite position in the VSAT centered coordinate frame  $\varphi_{\xi_\ell}^x$  and  $\varphi_{\xi_\ell}^y$ , as defined in (6), the elements of the autocorrelation matrix  $\mathbf{R}_{\mathbf{a}_{\ell,0}}$  are

$$\begin{aligned} [\mathbf{R}_{\mathbf{a}_{\ell,0}}]_{m,m'} &= \mathbb{E} \left\{ \exp \left( -jv \left( d_{A,m}^x \phi_\ell^x + d_{A,m}^y \phi_\ell^y \right. \right. \right. \\ &\quad \left. \left. \left. - d_{A,m'}^x \phi_\ell^x - d_{A,m'}^y \phi_\ell^y \right) \right) \right\} \end{aligned}$$

$$\begin{aligned} &= \exp \left( -jv \left( \left( d_{A,m}^x - d_{A,m'}^x \right) \hat{\phi}_\ell^x \right. \right. \\ &\quad \left. \left. + \left( d_{A,m}^y - d_{A,m'}^y \right) \hat{\phi}_\ell^y \right) \right) \\ &\quad \cdot \varphi_{\xi_\ell}^x \left( v \left( d_{A,m}^x - d_{A,m'}^x \right) \right) \\ &\quad \cdot \varphi_{\xi_\ell}^y \left( v \left( d_{A,m}^y - d_{A,m'}^y \right) \right). \end{aligned} \quad (41)$$

Furthermore, let  $f_{\tilde{\phi}_{\ell,\ell'}}^x(\tilde{\phi}_{\ell,\ell'}^x) \in \mathbb{R}$  and  $f_{\tilde{\phi}_{\ell,\ell'}}^y(\tilde{\phi}_{\ell,\ell'}^y) \in \mathbb{R}$  be the PDFs for the space angles of the incoming waves at the  $\ell'$ th NLoS path in x- and y-direction. Then, the elements of the corresponding correlation matrix  $\mathbf{R}_{\tilde{\mathbf{a}}_\ell} = \mathbb{E}\{\tilde{\mathbf{a}}_\ell \tilde{\mathbf{a}}_\ell^H\}$  are

$$\begin{aligned} [\mathbf{R}_{\tilde{\mathbf{a}}_\ell}]_{m,m'} &= \sum_{\ell'=1}^{L_p} \mathbb{E} \left\{ |\tilde{\alpha}_{\ell'}|^2 \right. \\ &\quad \cdot \exp \left( -jv \left( d_{A,m}^x \tilde{\phi}_{\ell,\ell'}^x + d_{A,m}^y \tilde{\phi}_{\ell,\ell'}^y \right. \right. \\ &\quad \left. \left. - d_{A,m'}^x \tilde{\phi}_{\ell,\ell'}^x - d_{A,m'}^y \tilde{\phi}_{\ell,\ell'}^y \right) \right) \left. \right\} \\ &= \sum_{\ell'=1}^{L_p} \tilde{\sigma}_{\alpha_{\ell,\ell'}}^2 \varphi_{\tilde{\phi}_{\ell,\ell'}}^x \left( v \left( d_{A,m'}^x - d_{A,m}^x \right) \right) \\ &\quad \cdot \varphi_{\tilde{\phi}_{\ell,\ell'}}^y \left( v \left( d_{A,m'}^y - d_{A,m}^y \right) \right), \end{aligned} \quad (42)$$

where  $\varphi_{\tilde{\phi}_{\ell,\ell'}}^x(\cdot)$  and  $\varphi_{\tilde{\phi}_{\ell,\ell'}}^y(\cdot)$  are the CFs for the space angles  $\tilde{\phi}_{\ell,\ell'}^x$  and  $\tilde{\phi}_{\ell,\ell'}^y$ , respectively. With (12), the autocorrelation matrix for the array response vector  $\mathbf{a}_\ell$  is

$$\mathbf{R}_{\mathbf{a}_\ell} = \frac{\kappa_\ell}{\kappa_\ell + 1} \mathbf{R}_{\mathbf{a}_{\ell,0}} + \frac{1}{\kappa_\ell + 1} \mathbf{R}_{\tilde{\mathbf{a}}_\ell}. \quad (43)$$

Correspondingly, the channel correlation matrix (40) can be equivalently written as  $\mathbb{E}\{\mathbf{H}_\ell \mathbf{H}_\ell^H\} = \sigma_{\alpha_\ell}^2 N_t \mathbf{R}_{\mathbf{a}_\ell}$ .

A solution to this optimization problem is stated next.

*Proposition 3:* The receive vector  $\mathbf{w}_{\ell, \text{opt}}$  for satellite  $\ell$  that maximizes the mean SINR is proportional to the eigenvector corresponding to the largest eigenvalue of  $(\sum_{i \neq \ell} \tilde{\sigma}_{\alpha_i}^2 \mathbf{R}_{\mathbf{a}_i} + \sigma_n^2 \mathbf{I}_{N_r})^{-1} \mathbf{R}_{\mathbf{a}_\ell}$ , where  $\tilde{\sigma}_{\alpha_i}^2 = \sigma_{\alpha_i}^2 \mathbb{E}\{|\mathbf{b}_i^H \mathbf{g}_i|^2\}$  is the mean received signal power from satellite  $i$ .

*Proof:* Plugging (10) into the objective function in (39) gives

$$\mathbb{E} \left\{ \frac{|\alpha_\ell \mathbf{w}_\ell^H \mathbf{a}_\ell \mathbf{b}_\ell^H \mathbf{g}_\ell|^2}{\sum_{i \neq \ell} |\alpha_i \mathbf{w}_\ell^H \mathbf{a}_i \mathbf{b}_i^H \mathbf{g}_i|^2 + \sigma_n^2 \mathbf{w}_\ell^H \mathbf{w}_\ell} \right\} \quad (44a)$$

$$= \frac{\sigma_{\alpha_\ell}^2 \mathbf{w}_\ell^H \mathbb{E}\{\mathbf{a}_\ell \mathbf{b}_\ell^H \mathbf{g}_\ell \mathbf{g}_\ell^H \mathbf{b}_\ell \mathbf{a}_\ell\} \mathbf{w}_\ell}{\sum_{i \neq \ell} \sigma_{\alpha_i}^2 \mathbf{w}_\ell^H \mathbb{E}\{\mathbf{a}_i \mathbf{b}_i^H \mathbf{g}_i \mathbf{g}_i^H \mathbf{b}_i \mathbf{a}_i\} \mathbf{w}_\ell + \sigma_n^2 \mathbf{w}_\ell^H \mathbf{w}_\ell} \quad (44b)$$

$$= \frac{\tilde{\sigma}_{\alpha_\ell}^2 \mathbf{w}_\ell^H \mathbb{E}\{\mathbf{a}_\ell \mathbf{a}_\ell^H\} \mathbf{w}_\ell}{\mathbf{w}_\ell^H \left( \sum_{i \neq \ell} \tilde{\sigma}_{\alpha_i}^2 \mathbb{E}\{\mathbf{a}_i \mathbf{a}_i^H\} + \sigma_n^2 \mathbf{I}_{N_r} \right) \mathbf{w}_\ell} \quad (44c)$$

$$= \tilde{\sigma}_{\alpha_\ell}^2 \cdot \frac{\mathbf{w}_\ell^H \mathbf{R}_{\mathbf{a}_\ell} \mathbf{w}_\ell}{\mathbf{w}_\ell^H \left( \sum_{i \neq \ell} \tilde{\sigma}_{\alpha_i}^2 \mathbf{R}_{\mathbf{a}_i} + \sigma_n^2 \mathbf{I}_{N_r} \right) \mathbf{w}_\ell}. \quad (44d)$$

Observe that this is a generalized Rayleigh quotient. By virtue of Lemma 1 in Appendix B, (44d) is maximized if

$\mathbf{w}_\ell$  is proportional to an eigenvector corresponding to the maximum eigenvalue of  $(\sum_{i \neq \ell} \bar{\sigma}_{\alpha_i}^2 \mathbf{R}_{\mathbf{a}_i} + \sigma_n^2 \mathbf{I}_{N_r})^{-1} \mathbf{R}_{\mathbf{a}_\ell}$ . ■

Similar to the optimal precoder form Proposition 1, the optimal equalizer has no closed-form solution and requires a numerical eigendecomposition, in general. In the following subsection, closed-form solutions for the special case of perfect position are derived.

### C. PERFECT POSITION KNOWLEDGE

Given perfect position knowledge and pure LoS connection, i.e.,  $\Xi^{\mathbf{W}_\ell} = \xi_\ell^{\mathbf{W}} = 0 \Leftrightarrow \varphi_{\Xi^{\mathbf{W}_\ell}}(t) = \varphi_{\xi_\ell^{\mathbf{W}}}(t) = 1$  and  $\kappa_\ell \rightarrow \infty$  for all  $\ell$ , closed-form solutions for the optimal precoder (20) and equalizer (39) can be obtained. This closed-form solutions are then used to obtain heuristic precoder and equalizer with reduced complexity. In Corollary 1 and 2 the optimal precoder and equalizer for perfect position knowledge are stated, respectively.

*Corollary 1:* A precoder that maximizes the received signal power under per-satellite power constraint with perfect position knowledge is given by

$$\begin{aligned} \mathbf{G}_{\text{per}} &= \mathbf{G}_{\text{opt}} \Big|_{\substack{\Xi^{\mathbf{x}_\ell} = 0 \\ \Xi^{\mathbf{y}_\ell} = 0}} = \sqrt{\frac{\rho}{N_t}} \text{blkdiag}(\mathbf{b}_1, \dots, \mathbf{b}_{N_S}) \\ &= \text{blkdiag}(\mathbf{g}_{1,\text{per}}, \dots, \mathbf{g}_{N_S,\text{per}}). \end{aligned} \quad (45)$$

*Proof:* Given the general solution from Proposition 1, the precoding vector  $\mathbf{g}_{\ell,\text{per}}$  must be an eigenvector corresponding to the largest eigenvalue of  $\mathbf{R}_{\mathbf{b}_\ell}$ . For perfect position knowledge, we have  $\varphi_{\Xi^{\mathbf{W}_\ell}}(t) = 1$ , and correspondingly, the autocorrelation matrix reduces to

$$\mathbf{R}_{\mathbf{b}_\ell} \Big|_{\substack{\Xi^{\mathbf{x}_\ell} = 0 \\ \Xi^{\mathbf{y}_\ell} = 0}} = \mathbf{b}_\ell \mathbf{b}_\ell^H. \quad (46)$$

Thus,  $\mathbf{R}_{\mathbf{b}_\ell}$  becomes a rank one matrix with the eigenvector  $\mathbf{b}_\ell / \sqrt{N_t}$  corresponding to the only non-zero eigenvalue. Furthermore, scaling of the eigenvector is necessary to achieve the optimum in (20), such that  $\mathbf{g}_{\ell,\text{per}}^H \mathbf{g}_{\ell,\text{per}} = \rho$  holds. Correspondingly, an optimal precoding vector for satellite  $\ell$  with perfect position knowledge is  $\mathbf{g}_{\ell,\text{per}} = \sqrt{\rho / N_t} \mathbf{b}_\ell$ . ■

*Corollary 2:* Under pure LoS connection and perfect position knowledge, a linear equalizer  $\mathbf{w}_\ell$  that maximizes the mean SINR, i.e., a solution to (39), is

$$\begin{aligned} \mathbf{w}_{\ell,\text{per}} &= \lim_{\{\kappa_i\}_{i=1}^{N_S} \rightarrow \infty} \mathbf{w}_{\ell,\text{opt}} \Big|_{\substack{\{\xi_i^x\}_{i=1}^{N_S} = 0 \\ \{\xi_i^y\}_{i=1}^{N_S} = 0}} \\ &= \left( \mathbf{A}_0 \bar{\Sigma}_\alpha^2 \mathbf{A}_0^H + \sigma_n^2 \mathbf{I}_{N_r} \right)^{-1} \mathbf{a}_{\ell,0} \end{aligned} \quad (47)$$

where  $\bar{\Sigma}_\alpha^2 = \text{diag}(\bar{\sigma}_{\alpha_1}^2, \dots, \bar{\sigma}_{\alpha_{N_S}}^2)$  and  $\mathbf{A}_0 = [\mathbf{a}_{1,0}, \dots, \mathbf{a}_{N_S,0}]$ .

*Proof:* Under pure LoS connection, we have

$$\lim_{\kappa_\ell \rightarrow \infty} \mathbf{R}_{\mathbf{a}_\ell} = \mathbf{R}_{\mathbf{a}_{\ell,0}}. \quad (48)$$

With perfect position knowledge, the autocorrelation further simplifies to

$$\mathbf{R}_{\mathbf{a}_{\ell,0}} \Big|_{\substack{\xi_\ell^x = 0 \\ \xi_\ell^y = 0}} = \mathbf{a}_{\ell,0} \mathbf{a}_{\ell,0}^H. \quad (49)$$

Correspondingly,  $\mathbf{w}_{\ell,\text{per}}$  must be proportional to the eigenvector corresponding to the largest eigenvalue of

$$\begin{aligned} &\left( \sum_{i \neq \ell} \bar{\sigma}_{\alpha_i}^2 \mathbf{R}_{\mathbf{a}_i} + \sigma_n^2 \mathbf{I}_{N_r} \right)^{-1} \mathbf{R}_{\mathbf{a}_\ell} \Big|_{\substack{\xi_\ell^x = 0 \\ \xi_\ell^y = 0}} \\ &= \left( \sum_{i \neq \ell} \bar{\sigma}_{\alpha_i}^2 \mathbf{a}_{i,0} \mathbf{a}_{i,0}^H + \sigma_n^2 \mathbf{I}_{N_r} \right)^{-1} \mathbf{a}_{\ell,0} \mathbf{a}_{\ell,0}^H \\ &= \left( \mathbf{A}_0 \bar{\Sigma}_\alpha^2 \mathbf{A}_0^H + \sigma_n^2 \mathbf{I}_{N_r} \right)^{-1} \mathbf{a}_{\ell,0} \mathbf{a}_{\ell,0}^H. \end{aligned} \quad (50)$$

It is established in [73, Sec. 3] that (47) is such an eigenvector. ■

Note that any  $\beta \mathbf{w}_{\ell,\text{per}}$ , with  $\beta \neq 0$ , is a valid solution for (39). Common choices are  $\beta = 1$  [10], or  $\beta = 1 / |\mathbf{w}_{\ell,\text{per}}^H \mathbf{H}_\ell \mathbf{g}_\ell|$  [41], [43]. However, such a scaling factor  $\beta$  is only for the purpose of normalization and has no impact on the SINR or the achievable rate.

Given the closed-form solutions (45) and (47), we obtain the heuristic precoder  $\mathbf{g}_{\ell,\text{heu}}$  and equalizer  $\mathbf{w}_{\ell,\text{heu}}$  as an approximation of  $\mathbf{g}_{\ell,\text{per}}$  and  $\mathbf{w}_{\ell,\text{per}}$ , respectively,

$$\mathbf{g}_{\ell,\text{heu}} = \sqrt{\frac{\rho}{N_t}} \hat{\mathbf{b}}_\ell \quad (51)$$

$$\mathbf{w}_{\ell,\text{heu}} = \left( \hat{\mathbf{A}} \bar{\Sigma}_\alpha^2 \hat{\mathbf{A}}^H + \sigma_n^2 \mathbf{I}_{N_r} \right)^{-1} \hat{\mathbf{a}}_\ell, \quad (52)$$

where  $\hat{\mathbf{A}} = [\hat{\mathbf{a}}_1, \dots, \hat{\mathbf{a}}_{N_S}]$  and the elements of the estimated steering vector are  $[\hat{\mathbf{a}}_\ell]_m = \exp(j\nu(d_{A,m}^x \hat{\phi}_\ell^x + d_{A,m}^y \hat{\phi}_\ell^y))$ . Stacking the individual equalizer  $\{\mathbf{w}_{i,\text{heu}}\}_{i=1}^{N_S}$  gives the overall equalizer matrix

$$\begin{aligned} \mathbf{W}_{\text{heu}} &= \hat{\mathbf{A}}_0^H \left( \hat{\mathbf{A}} \bar{\Sigma}_\alpha^2 \hat{\mathbf{A}}^H + \sigma_n^2 \mathbf{I}_{N_r} \right)^{-1} \\ &= \left( \bar{\Sigma}_\alpha^2 \hat{\mathbf{A}}^H \hat{\mathbf{A}} + \sigma_n^2 \mathbf{I}_{N_S} \right)^{-1} \hat{\mathbf{A}}^H. \end{aligned} \quad (53)$$

The heuristic precoder (51) and equalizer (53) are suboptimal in general, but have reduced complexity compared to the optimal choices as they do not require eigendecompositions and can be directly obtained from the estimated positions. Furthermore, the heuristic precoding vector is based on manipulating only the phase at each antenna, and thus, an efficient implementation with a single RF chain per satellite is possible [33].

### IV. OPTIMAL INTER-SATELLITE DISTANCE

In this section, the impact of the inter-satellite distance on the achievable rate is discussed. In order to keep it mathematically tractable, the following simplifying assumptions are necessary:

- The VSAT is equipped with a uniform rectangular array (URA) of  $N_r = N_r^x \times N_r^y$  antennas spaced  $d_A$  apart.
- The transmit signal is precoded via a block diagonal matrix  $\mathbf{G} = \text{blkdiag}(\mathbf{g}_1, \dots, \mathbf{g}_{N_S})$ .
- The power from the NLoS parts is negligibly small, i.e.,  $\kappa_\ell \rightarrow \infty$  for all  $\ell$ .

- The channel matrices  $\mathbf{H}_\ell = \alpha_\ell \mathbf{a}_\ell \mathbf{b}_\ell^H$  are deterministic for all  $\ell$ .
- The received signal power from each satellite is the same, i.e.,  $|\alpha_i \mathbf{b}_i^H \mathbf{g}_i|^2 = |\alpha_\ell \mathbf{b}_\ell^H \mathbf{g}_\ell|^2 = \bar{\sigma}_\alpha^2$ .

Although, these are strong assumptions that do not hold in practical systems, it is shown via simulations in Section V that the derived optimal inter-satellite distance provides a good heuristic for the design of satellite swarms for high-throughput communications.

#### A. MAXIMIZATION OF THE ACHIEVABLE RATE

Assuming perfect CSI at the receiver (CSIR), and given the above mentioned assumptions, the achievable rate  $R_{\text{pc}}$  with a fixed precoder is

$$\begin{aligned} R_{\text{pc}} &= \log_2 \left| \mathbf{I}_{N_r} + \frac{1}{\sigma_n^2} \mathbf{H} \mathbf{G} \mathbf{G}^H \mathbf{H}^H \right| \\ &= \log_2 \left| \mathbf{I}_{N_r} + \frac{\bar{\sigma}_\alpha^2}{\sigma_n^2} \mathbf{A} \mathbf{A}^H \right|. \end{aligned} \quad (54)$$

Thus, the achievable rate  $R_{\text{pc}}$  depends on the effective channel  $\mathbf{A} \propto \mathbf{H} \mathbf{G}$ . By choosing a proper inter-satellite distance  $D_S$ , the dependency of the steering vectors  $\{\mathbf{a}_\ell\}_{\ell=1}^{N_S}$  can be controlled. This can be used to tune matrix  $\mathbf{A}$  such that the achievable rate is maximized. Therefore, we aim to find an inter-satellite distance  $D_{S,\text{opt}}$  such that

$$D_{S,\text{opt}} \in \arg \max_{D_S} \log_2 \left| \mathbf{I}_{N_r} + \frac{\bar{\sigma}_\alpha^2}{\sigma_n^2} \mathbf{A} \mathbf{A}^H \right|. \quad (55)$$

Solving this optimization problem is difficult due to the lack of a clear functional relationship between  $\mathbf{A}$  and  $D_S$ . A sufficient optimality condition that partially characterizes the solution space of (55) is stated next.

*Proposition 4:* Let  $k \in \mathbb{N}$  be a positive integer that is no multiple of  $N_r^x$  or  $N_r^y$ , i.e.,  $k/N_r^x \notin \mathbb{Z} \vee k/N_r^y \notin \mathbb{Z}$ . The achievable rate (54) is maximized, if the space angles satisfy

$$\begin{aligned} \forall \ell : \forall i \neq \ell : |\phi_\ell^x - \phi_i^x| &= \frac{2\pi k}{vd_A N_r^x} \\ \vee \quad |\phi_\ell^y - \phi_i^y| &= \frac{2\pi k}{vd_A N_r^y}. \end{aligned} \quad (56)$$

*Proof:* Observe that (54) is equivalent to

$$\begin{aligned} R_{\text{pc}} &= \log_2 \left| \mathbf{I}_{N_r} + \frac{\bar{\sigma}_\alpha^2}{\sigma_n^2} \mathbf{A} \mathbf{A}^H \right| \\ &= \log_2 \left| \mathbf{I}_{N_S} + \frac{\bar{\sigma}_\alpha^2}{\sigma_n^2} \mathbf{A}^H \mathbf{A} \right| \\ &= \log_2 \left( \prod_{\ell=1}^{N_S} \left( 1 + \tilde{\lambda}_\ell \frac{\bar{\sigma}_\alpha^2}{\sigma_n^2} \right) \right) \end{aligned} \quad (57)$$

where  $\tilde{\lambda}_\ell$  are the positive eigenvalues of  $\mathbf{A}^H \mathbf{A}$  [59]. Keeping the trace of  $\mathbf{A}^H \mathbf{A}$  constant, this is maximized if all eigenvalues have the same value [74, Th. 2.21]. In other words, any  $N_S \times N_S$  matrix  $\mathbf{Z} = \mathbf{A}^H \mathbf{A}$  maximizing (57) has a single eigenvalue  $\tilde{\lambda}$  with multiplicity  $N_S$ .

Further, observe that  $\mathbf{Z}$  is a normal matrix. By [75, Th. 2.5.4],  $\mathbf{Z}$  is similar to a diagonal matrix, i.e., there exists a nonsingular matrix  $\mathbf{S}$  such that  $\mathbf{S}^{-1} \Lambda \mathbf{S} = \mathbf{Z}$  with  $\Lambda$  diagonal. Since similar matrices have the same eigenvalues [75, Corollary 1.3.4],  $\Lambda$  must be  $\tilde{\lambda} \mathbf{I}$ . Then, for every nonsingular  $\mathbf{S}$ , we have  $\mathbf{Z} = \mathbf{S}^{-1} \tilde{\lambda} \mathbf{I} \mathbf{S} = \tilde{\lambda} \mathbf{S}^{-1} \mathbf{S} = \tilde{\lambda} \mathbf{I}$ . It follows that  $\mathbf{Z} = \tilde{\lambda} \mathbf{I}$  is the unique maximizer of (57). For  $\mathbf{A}^H \mathbf{A}$  to become a scaled identity matrix, its columns must satisfy  $\mathbf{a}_i^H \mathbf{a}_i = \tilde{\lambda}$  and  $\mathbf{a}_i^H \mathbf{a}_\ell = 0$  for all  $i$  and  $\ell \neq i$ .

For a URA at the VSAT, we can decompose the steering vector as  $\mathbf{a}_\ell = \mathbf{a}_\ell^x \otimes \mathbf{a}_\ell^y$ , where  $\mathbf{a}_\ell^x$  and  $\mathbf{a}_\ell^y$  are the steering vector components for the x- and y-direction. Consequently, we obtain

$$\begin{aligned} \mathbf{a}_i^H \mathbf{a}_\ell &= \left( \mathbf{a}_i^x \otimes \mathbf{a}_i^y \right)^H \left( \mathbf{a}_\ell^x \otimes \mathbf{a}_\ell^y \right) \\ &= \left( \mathbf{a}_i^x \right)^H \mathbf{a}_\ell^x \otimes \left( \mathbf{a}_i^y \right)^H \mathbf{a}_\ell^y \end{aligned} \quad (58)$$

This equals zero if  $(\mathbf{a}_i^x)^H \mathbf{a}_\ell^x$  or  $(\mathbf{a}_i^y)^H \mathbf{a}_\ell^y$  equals zero. Let  $|\phi_\ell^w - \phi_i^w| = \frac{2\pi k}{vd_A N_r^w}$ , the inner products on the right hand side of (58) becomes

$$\begin{aligned} (\mathbf{a}_i^w)^H \mathbf{a}_\ell^w &= \sum_{m=0}^{N_r^w-1} \exp(jvd_{Am}(\phi_\ell^w - \phi_i^w)) \\ &= \sum_{m=0}^{N_r^w-1} \exp\left(j \frac{2\pi mk}{N_r^w}\right) = 0. \end{aligned} \quad (59)$$

Finally, observe that

$$\begin{aligned} (\mathbf{a}_\ell^w)^H \mathbf{a}_\ell^w &= \sum_{m=0}^{N_r^w-1} \exp(jvd_{Am}(\phi_\ell^w - \phi_\ell^w)) \\ &= \sum_{m=0}^{N_r^w-1} \exp(0) = N_r^w. \end{aligned} \quad (60)$$

Thus, given the condition (56), the columns of  $\mathbf{A}$  are orthogonal, and therefore, the rate (54) is maximized. ■

Note that the difference of the space angles  $|\phi_\ell^w - \phi_i^w|$  increases monotonically with an increasing inter-satellite distance  $D_S$ . Therefore, the inter-satellite distance  $D_{S,\text{opt}}$  can be chosen such that (56) is satisfied, which maximizes the achievable rate according to Proposition 4. Furthermore, if (56) holds, the following relation between the optimal inter-satellite distance  $D_{S,\text{opt}}$  and the optimal precoder  $\mathbf{G}_{\text{per}}$  can be observed.

*Proposition 5:* The precoder  $\mathbf{G}_{\text{per}}$  in (45) achieves the upper bound (16) if (56) and  $|\alpha_i| = |\alpha_\ell| = |\alpha|$  for all  $i$  and  $\ell$  holds, i.e.,

$$\text{If (56)} \Rightarrow \mathbf{G}_{\text{per}} = \arg \max_{\text{tr}\{\mathbf{G}\mathbf{G}^H\} \leq N_S \rho} R_{\text{pc}} \quad (61)$$

*Proof:* First, recall that the channel  $\mathbf{H}$  can be decomposed as  $\mathbf{H} = \mathbf{A} \mathbf{S}_\alpha \mathbf{B}^H$ . Second, the upper bound achieving precoder is given by the scaled dominant right singular vectors of the channel matrix [59]. The SVD of the channel  $\mathbf{H}$  is defined as  $\mathbf{H} = \mathbf{U} \mathbf{S} \mathbf{V}^H$ , where  $\mathbf{U}$  and  $\mathbf{V}$  are unitary

matrices and  $\Sigma$  is a diagonal matrix with non-negative numbers on its main diagonal.

The complex-valued diagonal matrix  $\Sigma_\alpha$  is equivalent to

$$\begin{aligned}\Sigma_\alpha &= \text{diag}(|\alpha_1|, \dots, |\alpha_{N_S}|) \cdot \text{diag}(e^{-j\phi_1}, \dots, e^{-j\phi_{N_S}}) \\ &= \Sigma_{|\alpha|} \Sigma_\phi = \Sigma_\phi \Sigma_{|\alpha|}.\end{aligned}\quad (62)$$

Furthermore, due to the block diagonal structure of  $\mathbf{B}$ , we have  $\mathbf{B}^H \mathbf{B} = N_r \mathbf{I}_{N_S}$  and, if (56) holds, we also have  $\mathbf{A}^H \mathbf{A} = N_r \mathbf{I}_{N_S}$ . Thus, we can define the unitary matrices  $\mathbf{U}$  and  $\mathbf{V}$  as

$$\begin{aligned}\mathbf{U} &= \frac{1}{\sqrt{N_r}} [\mathbf{A}, \tilde{\mathbf{u}}_{N_S+1}, \dots, \tilde{\mathbf{u}}_{N_r^x}] \\ &\quad \cdot \begin{bmatrix} \Sigma_\phi & \mathbf{0}_{(N_r-N_S) \times (N_r-N_S)} \\ \mathbf{0}_{(N_r-N_S) \times (N_r-N_S)} & \mathbf{I}_{N_r-N_S} \end{bmatrix} \\ \mathbf{V} &= \frac{1}{\sqrt{N_t}} [\mathbf{B}, \tilde{\mathbf{v}}_{N_S+1}, \dots, \tilde{\mathbf{v}}_{N_{T_x}}]\end{aligned}\quad (63a)$$

where  $\{\tilde{\mathbf{u}}_{N_S+1}, \dots, \tilde{\mathbf{u}}_{N_r^x}\}$  and  $\{\tilde{\mathbf{v}}_{N_S+1}, \dots, \tilde{\mathbf{v}}_{N_{T_x}}\}$  are the left and right singular vectors belonging to the nullspace of  $\mathbf{H}$ , respectively. Consequently, the non-zero singular values are given by  $\{|\alpha_i|\}_{i=1}^{N_S}$ , i.e.,

$$\Sigma = \sqrt{N_r^x N_t} \begin{bmatrix} \Sigma_{|\alpha|} & \mathbf{0}_{N_S \times (N_{T_x} - N_S)} \\ \mathbf{0}_{(N_r^x - N_S) \times N_S} & \mathbf{0}_{(N_r^x - N_S) \times (N_{T_x} - N_S)} \end{bmatrix} \quad (64)$$

and the channel  $\mathbf{H}$  can be decomposed as

$$\begin{aligned}\mathbf{H} &= \mathbf{U} \Sigma \mathbf{V}^H = \mathbf{A} \Sigma_\phi \Sigma_{|\alpha|} \mathbf{B} \\ &= \sqrt{\frac{N_t}{\rho}} \mathbf{A} \Sigma_\phi \Sigma_{|\alpha|} \mathbf{G}_{\text{per}}.\end{aligned}\quad (65)$$

Therefore, the right singular vectors of  $\mathbf{H}$  are given by (45). Furthermore, if  $|\alpha_i| = |\alpha_\ell| = |\alpha|$  for all  $i$  and  $\ell$  holds, i.e.,  $\Sigma_{|\alpha|} = |\alpha| \mathbf{I}_{N_S}$ , then all precoding vectors  $\mathbf{g}_{\ell, \text{per}}$  must have the same power in order to achieve the capacity. This is given by the proposed precoder, as  $\|\mathbf{g}_{\ell, \text{per}}\|_2^2 = \|\mathbf{g}_{i, \text{per}}\|_2^2 = \rho$  for all  $i$  and  $\ell$ . ■

Propositions 4 and 5 show that the precoder  $\mathbf{G}_{\text{per}}$  is optimal w.r.t. to the achievable rate for distinct setups. In general, the proposed precoder is only sub-optimal. However, the gap in performance between the proposed approach and the theoretical upper bound turns out to be negligible small given large inter-satellite distances and a dominant LoS connection, as shown in Section V. Furthermore, compared to the optimal SVD-based precoder, the requirements on CSI acquisition are considerably relaxed and there is no need for any inter-satellite communication in order to determine the precoder matrix.

With Proposition 4, we have a sufficient condition for the optimal inter-satellite distance  $D_{S, \text{opt}}$ . A closed-form solution can be obtained for special cases, as shown in the following.

## B. CLOSED-FORM SOLUTION

In this section, an analytical solution for the optimal inter-satellite distance is derived. To obtain a closed-form solution, further simplifications are necessary. In particular, we assume that the satellite swarm is flying in a trail formation

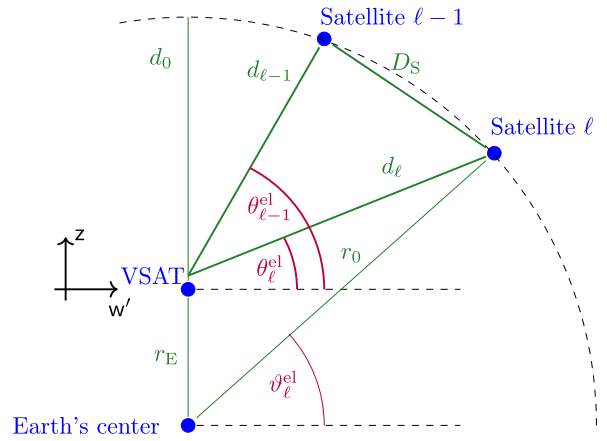


FIGURE 2. Geometric relation between two Satellites,  $\ell$  and  $\ell - 1$ , and the VSAT for  $\theta_\ell^{az} = \theta_{\ell-1}^{az} \in [0, \pi/2]$ .

with constant inter-satellite spacing  $D_S$ . This implies that the satellites follow a common orbit with altitude  $d_0$ . Furthermore, the orbital plane is perfectly aligned with either the  $x$ - or the  $y$ -axis of the VSAT-centered coordinate frame. Therefore, either  $\phi_\ell^x = 0$  or  $\phi_\ell^y = 0$  for  $\theta_\ell^{el} < \pi/2$ . In the following  $\mathbf{w}' \in \{\mathbf{x}, \mathbf{y}\}$  denotes that coordinate axis which is aligned with the orbital plane, i.e.,  $\phi_\ell^{\mathbf{w}'} \neq 0$  for  $\theta_\ell^{el} < \pi/2$ . Then, the VSAT's antenna array is effectively seen as a uniform linear array (ULA) with  $N_r^{\mathbf{w}'}$  antennas in the orbital plane.

Besides the VSAT-centered coordinate frame, we also require an Earth-centered coordinate frame whose  $\mathbf{w}'z$ -plane is aligned with the orbital plane. With the Earth's radius being  $r_E = 6371$  km, the orbital radius is  $r_0 = r_E + d_0$  and the position of satellite  $\ell$  in the Earth-centered coordinate frame is given by the triplet  $(r_0, \vartheta_\ell^{el}, \vartheta_\ell^{az})$ , whereas  $\vartheta_\ell^{az} \in [0, \pi/2]$ . The  $z$ -axis of the Earth centered coordinate frame is chosen to be aligned with the VSAT. Hence, the VSAT is located at position  $(r_E, \pi/2, 0)$ . This setup is illustrated in Fig. 2.

Considering the triangle between satellite  $\ell$ , the VSAT and the Earth's center as illustrated in Fig. 2, we obtain from the law of sines

$$\vartheta_\ell^{el} = \theta_\ell^{el} + \arcsin\left(\frac{r_E}{r_0} \cos(\theta_\ell^{el})\right) \quad (66)$$

$$d_\ell = r_0 \frac{\cos(\vartheta_\ell^{el})}{\cos(\theta_\ell^{el})}. \quad (67)$$

Then, the inter-satellite distance  $D_S$  is obtained from the law of cosines as

$$D_S = \sqrt{d_\ell^2 + d_{\ell-1}^2 - 2d_\ell d_{\ell-1} \cos(\theta_{\ell-1}^{el} - \theta_\ell^{el})} \quad (68)$$

where  $\vartheta_{\ell-1}^{el}$  and  $d_{\ell-1}$  are given analogously to (66) and (67), respectively.

Consider now two neighbouring satellites  $\ell$  and  $\ell - 1$ . According to Proposition 4, and given the above mentioned

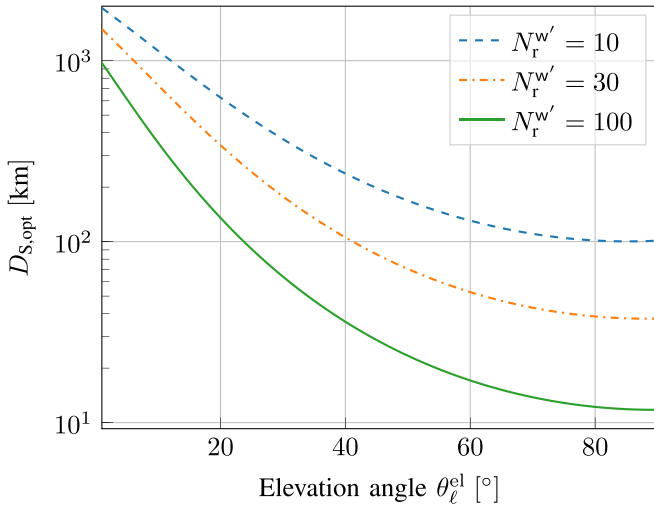


**FIGURE 3.** Optimal inter-satellite distances  $D_{S,\text{opt}}$  in dependence of the elevation angle  $\theta_\ell^{\text{el}}$ .

assumption  $\theta_\ell^{\text{az}} = \theta_{\ell-1}^{\text{az}} \in \{0, \pi/2\}$ , the first maximum is achieved if

$$\frac{2\pi}{\nu d_A N_r^{w'}} = \left| \cos(\theta_\ell^{\text{el}}) - \cos(\theta_{\ell-1}^{\text{el}}) \right| \Leftrightarrow \quad (69a)$$

$$\theta_{\ell-1} = \begin{cases} \arccos\left(\cos(\theta_\ell^{\text{el}}) - \frac{2\pi}{\nu d_A N_r^{w'}}\right) & \text{for } \cos(\theta_\ell^{\text{el}}) \geq \cos(\theta_{\ell-1}^{\text{el}}) \\ \arccos\left(\frac{2\pi}{\nu d_A N_r^{w'}} - \cos(\theta_\ell^{\text{el}})\right) & \text{for } \cos(\theta_{\ell-1}^{\text{el}}) \geq \cos(\theta_\ell^{\text{el}}). \end{cases} \quad (69b)$$

Then, plugging (69b) in (66) and then in (67) and (68), respectively, one gets a solution for the optimal inter-satellite distance  $D_{S,\text{opt}}$ , which depends on the altitude  $d_0$ , the elevation angle  $\theta_\ell^{\text{el}}$  of satellite  $\ell$ , the number of receive antennas  $N_r^{w'}$  and the antenna spacing  $d_A$  at the VSAT, as well as the wavenumber  $\nu$ . As there is little intuition to be gained from the explicit formula for  $D_{S,\text{opt}}$  (79) shown at the top of the p. 17, it is delegated to Appendix C.

In Fig. 3 and 4, the dependency between the optimum inter-satellite distance  $D_{S,\text{opt}}$ , the elevation angle  $\theta_\ell^{\text{el}}$  and number of receive antennas  $N_r^{w'}$  is shown for an altitude  $d_0 = 600$  km and  $\nu d_A = \pi$ . Note that, according to (56), the product  $\nu d_A N_r^{w'}$  determines the spatial resolution. Therefore, increasing the antenna spacing  $d_A$  by a certain factor and decreasing the number of antennas  $N_r^{w'}$  by the same factor, gives the same results.

It can be seen in Fig. 3 that the optimum inter-satellite distance  $D_{S,\text{opt}}$  increases strongly as the elevation angle  $\theta_\ell^{\text{el}}$  decreases. However, the satellites have distinct elevation angles, i.e.,  $\theta_\ell^{\text{el}} \neq \theta_i^{\text{el}}$  for all  $i \neq \ell$ . This means that the optimal distance between satellites  $i$  and  $i-1$  is different to the optimal distance between satellite  $\ell$  and  $\ell-1$ . Furthermore, the elevation angles changes over time. Thus, it is not possible to ensure orthogonal steering vectors between all satellites, i.e.,  $\mathbf{a}_i^H \mathbf{a}_\ell = 0$  for all  $i \neq \ell$ , during the whole flight with a constant inter-satellite distance

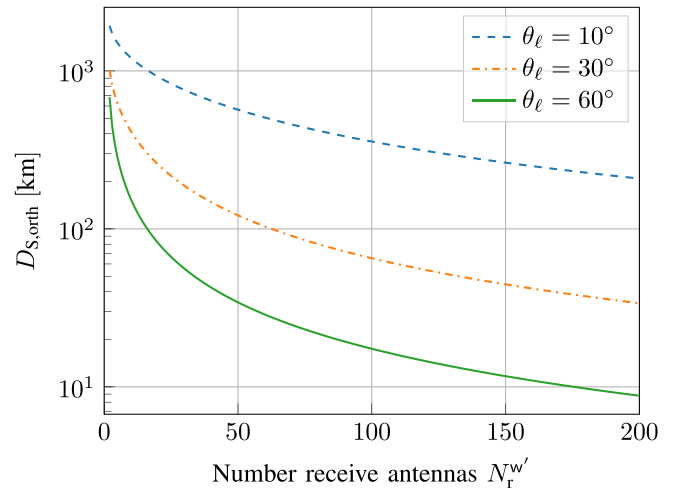


**FIGURE 4.** Optimal inter-satellite distances  $D_{S,\text{opt}}$  in dependence of the number of receive antennas  $N_r^{w'}$ .

$D_S$ . Adjusting the inter-satellite distance during the flight, however, requires additional fuel and increased complexity for flight control and should thus be avoided. Nevertheless, as evaluated numerically in Section V, the channel capacity is not decreasing much after the first local optimum and, thus, a close-to-optimal heuristic is obtained by relaxing condition (56). In particular, the average rate over the whole flight is close to maximum if

$$\min_\ell \left| \cos(\theta_\ell^{\text{el}}) - \cos(\theta_{\ell-1}^{\text{el}}) \right| \geq \frac{2\pi}{\nu d_A N_r^{w'}} \quad (70)$$

holds during the transmission. This can be used as a rule of thumb to find a proper inter-satellite distance  $D_S$ , if the minimum elevation angle is known a priori.

## V. NUMERICAL EVALUATIONS

In Section IV, it has been shown theoretically, that the proposed transceiver design is optimal w.r.t. the achievable rate for distinct setup. In the following, simulation results are presented to provide insight about how close the proposed transceiver is to optimum under practical assumptions. The considered performance metric is the achievable rate  $R_{\text{lin}}$  as defined in (37). Since most SotA precoder approaches for satellite swarms focus only on handheld connectivity, the upper bound  $R_{\text{opt}} \geq R_{\text{lin}}$ , as presented in Section II-C, is considered as the only benchmark.

First, the performance of the robust approach and the heuristic one are compared. Then, the impact of the Rician factors  $\{\kappa_\ell\}_{\ell=1}^{N_S}$  and the inter-satellite distance  $D_S$  is further analyzed. Throughout the simulations, two different satellite swarms are considered. One is a swarm with  $N_S = 3$  satellites forming an equilateral triangle with distance  $D_S$  between any of the satellites. The other swarm consists of  $N_S = 4$  satellites, forming a square where each side has the length  $D_S$ . For a fair comparison we consider the sum transmit power  $P_{\text{Tx}}$  over all satellites. Thus, the transmit power of each satellite is  $\rho = P_{\text{Tx}}/N_S$ . The parameters

**TABLE 2.** Simulation setup parameters.

Parameter	Symbol	Value
Number receive antennas	$N_r$	256
Number satellites	$N_s$	{3, 4}
Number transmit antennas per satellite	$N_t$	64
Receive antenna gain per element	$\zeta_{R_x, \text{dB}}$	15.6 dBi
Transmit antenna gain per element	$\zeta_{T_x, \text{dB}}$	{15.7 dBi, 14.4 dBi}
Receive antenna spacing	$d_A$	3.75 cm
Transmit antenna spacing	$D_A$	3.75 cm
Minimum elevation angle	$\theta_{\min}$	$30^\circ$
Carrier frequency	$f_c$	20 GHz
Altitude	$d_0$	600 km
Noise power	$P_{N, \text{dB}}$	-120 dBW

used during the simulations are summarized in Table 2. The antenna gains  $\zeta_{R_x, \text{dB}}$  and  $\zeta_{T_x, \text{dB}}$  are chosen such that the total array gain matches the 3GPP recommendations, i.e.,  $\zeta_{R_x, \text{dB}} + 10 \log_{10}(N_r) = 39.7 \text{ dBi}$  and  $\zeta_{T_x, \text{dB}} + 10 \log_{10}(N_s N_t) = 38.5 \text{ dBi}$  [76]. Furthermore, the antenna arrays at the satellites and the VSAT are URAs with  $N_r^x = N_r^y = \sqrt{N_r}$  and  $N_t^x = N_t^y = \sqrt{N_t}$  antennas along each dimension, respectively. The magnitude of the channel  $|\alpha_\ell|^2$  is chosen according to the rural scenario specified by 3GPP in [55].

To get insights about how the NLoS paths impacts the performance of the proposed position based transceiver design, we assume that the NLoS paths are considered to arrive from all possible directions with the same power. This is a worst case scenario, since the correlation matrices for NLoS parts become the identity matrix, i.e.,  $\mathbf{R}_{\mathbf{a}_\ell} = \mathbf{I}_{N_r}$ . Therefore, there are no useful information about the direction of the NLoS parts available to improve the performance. Furthermore, we assume the same Rician factor  $\kappa = \kappa_\ell$  for all  $\ell$ .

### A. IMPACT OF POSITION KNOWLEDGE

In this subsection, the performance of the derived precoder and equalizer, as introduced in Section III, are evaluated. During the simulations an inter-satellite distance of  $D_s = 50 \text{ km}$  is assumed and the position estimation error is assumed to be uniformly distributed in the interval  $[-\delta_{\max}, \delta_{\max}]$ , for the satellites as well as the ground station and in both x- and y-direction. The Rician factors are set as  $\kappa = 10$ . The corresponding achievable rates are shown in Fig. 5 and 6 w.r.t. the sum transmit power  $P_{T_x}$  for  $N_s \in \{3, 4\}$  satellites. The robust approach denotes the precoder and equalizer from propositions 1 and 3, while the heuristic approach refers to the low complexity approximations (51) and (53), respectively.

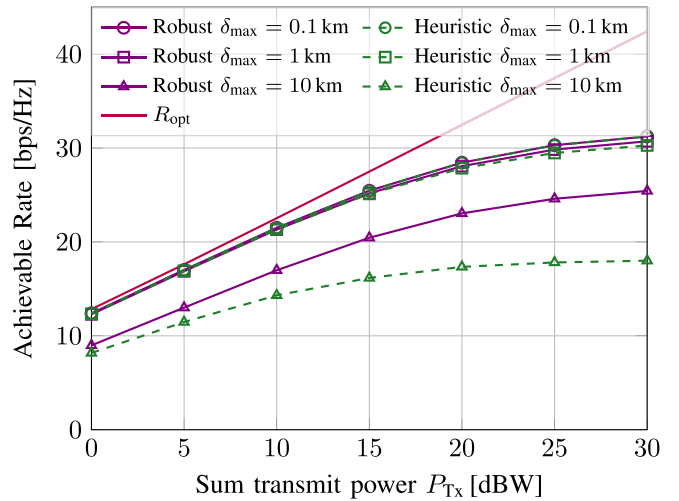


**FIGURE 5.** Achievable rate performance for  $N_s = 3$  satellites.

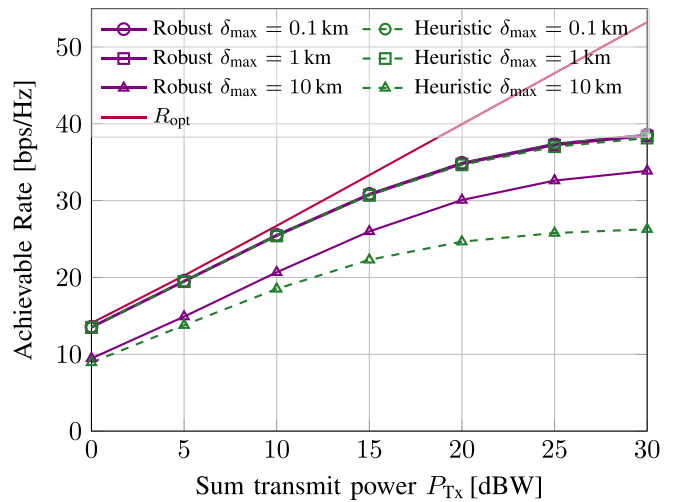


**FIGURE 6.** Achievable rate performance for  $N_s = 4$  satellites.

Both approaches are close to the upper bound  $R_{\text{opt}}$  (16) for small position uncertainties, i.e., if  $\delta_{\max} \leq 1 \text{ km}$ , and practically relevant transmit powers. For large position uncertainties, the robust approach shows a clear performance gain over the heuristic approach. These observations are independent of the number of satellites, while with  $N_s = 4$  satellites higher data rates are achieved compared to  $N_s = 3$  satellites. For very large transmit powers, the impact of the NLoS paths limits the achievable rate and the gap to the upper bound  $R_{\text{opt}}$  increases. Since the NLoS paths may arrive from any direction with the same probability, independent of the satellites' position, efficient equalization of the NLoS components solely based on positional information is not possible. Therefore, with increasing transmit power, the interference power increases, too. Such performance degradation in the high SNR regime is also a common observation if the estimated channel is disturbed by an additive error [35], [36]

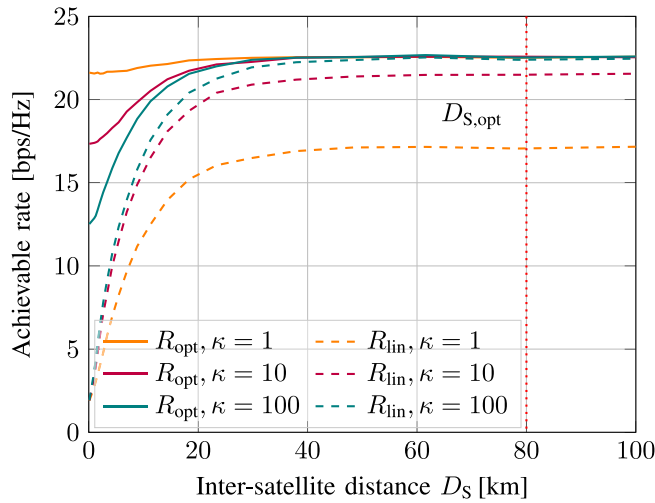


FIGURE 7. Achievable rate performance in dependence of inter-satellite distances  $D_S$  for  $N_s = 3$  satellites.

### B. IMPACT OF RICIAN FACTOR AND INTER-SATELLITE DISTANCE

In Section IV, the optimal inter-satellite distance  $D_{S,opt}$  under simplifying assumptions has been derived. According to that derivation and given the simulation parameter from Table 2, the optimal inter-satellite distance is  $D_{S,opt} = 80$  km. In Fig. 7 and 8, the achievable rates for different inter-satellite distances and Rician factors  $\kappa$  are shown. The sum transmit power of the satellite swarms has been set to  $P_{Tx} = 10$  W and perfect position knowledge has been assumed. In this case the performance differences between the heuristic and robust approach are indistinguishable.

It can be seen that the upper bound  $R_{opt}$ , denoted by the solid lines, as well as the achievable rate with the proposed transceiver design, denoted by the dashed lines, increase with increasing inter-satellite distance up to a certain point. Furthermore, the upper bound can be achieved for large Rician factors, i.e., for dominant LoS paths, and large inter-satellite distances.

Note that for decreasing Rician factors, the performance of the proposed transceiver decreases, as there is less deterministic CSI available at the receiver. However, the upper bound for small inter-satellite distances increases with a decreasing Rician factor  $\kappa$ . This is due to the fact that the NLoS paths are uncorrelated, and therefore, the channel matrix  $\mathbf{H}$  is well conditioned, even for small inter-satellite distances. Furthermore, the overall path loss is independent of the Rician factor during the simulations. This does not hold in real world applications. Usually, a small Rician factor implies weak LoS connection, and therefore, a higher path loss. Therefore, satellite communication with a small Rician factor is usually not possible. Instead, high Rician factors are common in satellite communication [55]. Thus, the inter-satellite distance  $D_{S,opt}$ , as derived in Section IV, provides a promising guideline for inter-satellite distances in satellite swarms, and the proposed position based transceiver shows good performance around  $D_{S,opt}$ .

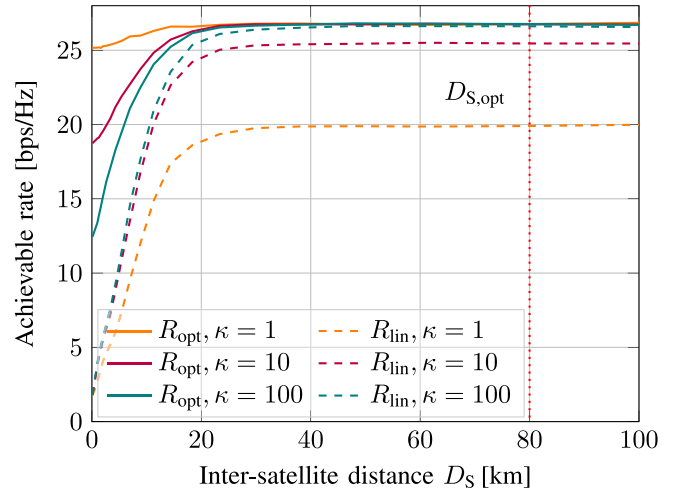


FIGURE 8. Achievable rate performance in dependence of inter-satellite distances  $D_S$  for  $N_s = 4$  satellites.

### VI. CONCLUSION

The advancement in formation flying over the past years allows to connect multiple small satellites to a satellite swarm, which enables increased spectral efficiencies compared to monolithic satellites. In this paper, we have shown that high data rates in the downlink can be already achieved with relatively low complexity, making satellite swarms a promising solution to provide high data rates in future NTN. In particular, a low complexity distributed precoder and a linear equalizer, both utilizing the geometric relation between the positions of the satellites and VSAT, has been proposed. The requirements for channel estimation are very low, as only relative positional knowledge between the satellites and the VSAT as well as long term statistics of the channel are necessary. Furthermore, an approach to optimize the inter-satellite distance has been presented. Given that the inter-satellite distance is chosen adequately, the proposed transceiver combination achieves the theoretical upper bound of the achievable rate, without the necessity of any time-critical inter-satellite communication, if a dominant LoS path is present and the position uncertainty is small. Similar observations w.r.t. to the inter-satellite distance do also hold for the uplink. It has been observed in [2], that the gain due to joint processing among the satellites of the received signals is negligible small compared to only individual processing of the received signal, if the proposed inter-satellite distance is chosen.

Although, the proposed precoder does not require phase alignment among the satellites, frequency and time synchronization is still a non-trivial task. In particular, if the inter-satellite distances are very large and multiple VSATs are to be served, each satellite-to-VSAT link experiences a different Doppler shift and different delay. Therefore, further studies on synchronization in satellite swarms are required, especially for multi-user scenarios.

Furthermore, the presented approach is only optimal for VSATs, which can make use of relatively large antenna

arrays compared to handhelds. Since future satellite constellations should be able to serve handhelds and VSATs, designing satellite swarms and flexible precoding approaches to serve both types of user equipment is subject of future studies.

In order to provide global coverage, a constellation consisting of several satellite swarms is required. Such a constellation of satellite swarms brings further challenges due to the increased number of satellites, e.g., the complexity for routing and handover increases due to the large number of network nodes, and operating the large number of satellites and handling the space debris becomes more challenging.

## APPENDIX A SYSTEM MODEL WITH MULTIPLE SYNCHRONIZATION CIRCUITS AT VSAT

Throughout the paper, a single circuit at the VSAT has been assumed to synchronize with the satellites. In Section II-D.2, the use of multiple synchronization circuits has been proposed as an alternative approach with hardware costs at the VSAT but with less inter-satellite communication. In the following, it is shown how to adapt the system model for multiple synchronization circuits.

With  $N_S$  synchronization circuits, the VSAT can synchronize with each satellite independently, e.g., by assigning different spreading codes to the satellites [77]. After compensating the timing and frequency offsets, the output of each synchronization circuit is different. Let the  $\ell$ th circuit of the VSAT be synchronized with the  $\ell$ th satellite, the  $\ell$ th output signal  $\mathbf{y}_\ell \in \mathbb{C}^{N_r}$  is given by

$$\mathbf{y}_\ell = \mathbf{H}_\ell \mathbf{x}_\ell + \sum_{\substack{i=1 \\ i \neq \ell}}^{N_S} \mathbf{H}_i \mathbf{x}_i \exp(j\varepsilon_{\ell,i}) + \mathbf{n}_\ell, \quad (71)$$

where  $\varepsilon_{\ell,i}$  is the phase shift at the  $\ell$ th output due to the incorrect timing and frequency compensation of the  $i$ th satellites' signal.

Following the proposed approach that each satellite transmits an independent data stream, the  $\ell$ th estimated stream  $\hat{s}_\ell$  is given by

$$\hat{s}_\ell = \mathbf{w}_\ell^H \mathbf{y}_\ell. \quad (72)$$

Since the phase shift  $\varepsilon_{\ell,i}$  doesn't affect the received signal power, i.e.,

$$\begin{aligned} \mathbb{E} \left\{ \left| \mathbf{w}_\ell^H \mathbf{H}_i \mathbf{x}_i \exp(j\varepsilon_{\ell,i}) \right|^2 \right\} &= \mathbb{E} \left\{ \left| \mathbf{w}_\ell^H \mathbf{H}_i \mathbf{x}_i \right|^2 \right\} \\ &= \left| \mathbf{w}_\ell^H \mathbf{H}_i \mathbf{g}_i \right|^2, \end{aligned} \quad (73)$$

the linear equalizer  $\mathbf{w}_\ell$  can be determined in the same way as shown in Section III-B. However, the vectors can't be stacked to a joint equalization matrix  $\mathbf{W}$  because each  $\mathbf{w}_\ell$  is applied to an individual receive signal  $\mathbf{y}_\ell \neq \mathbf{y}_i$ .

## APPENDIX B GENERALIZED RAYLEIGH QUOTIENT

*Lemma 1:* Let  $\mathbf{A} \in \mathbb{C}^{n \times n}$  be Hermitian and  $\mathbf{B} \in \mathbb{C}^{n \times n}$  Hermitian positive definite. Then,

$$\max_{\mathbf{x} \in \mathbb{C}^n \setminus \{0\}} \frac{\mathbf{x}^H \mathbf{A} \mathbf{x}}{\mathbf{x}^H \mathbf{B} \mathbf{x}} = \lambda_{\max}(\mathbf{A}, \mathbf{B}), \quad (74)$$

where  $\lambda_{\max}(\mathbf{A}, \mathbf{B})$  is the maximum generalized eigenvalue. The optimal  $\mathbf{x}$  in (74) is an eigenvector corresponding to  $\lambda_{\max}(\mathbf{A}, \mathbf{B})$ .

*Proof:* Let  $\mathbf{L}\mathbf{L}^H$  be the Cholesky factorization of  $\mathbf{B}$ . Substitute  $\mathbf{y} = \mathbf{L}^H \mathbf{x}$  in (74). Then,

$$\begin{aligned} \max_{\mathbf{x} \in \mathbb{C}^n \setminus \{0\}} \frac{\mathbf{x}^H \mathbf{A} \mathbf{x}}{\mathbf{x}^H \mathbf{L}\mathbf{L}^H \mathbf{x}} &= \max_{\mathbf{y} \in \mathbb{C}^n \setminus \{0\}} \frac{\mathbf{y}^H \mathbf{L}^{-1} \mathbf{A} \mathbf{L}^{-H} \mathbf{y}}{\mathbf{y}^H \mathbf{y}} \\ &= \lambda_{\max}(\mathbf{L}^{-1} \mathbf{A} \mathbf{L}^{-H}), \end{aligned} \quad (75)$$

where the last step is due to the Rayleigh-Ritz Theorem [75, Th. 4.2.2].

Recall that two square matrices  $\mathbf{C}, \mathbf{D}$  are similar if there exists a nonsingular matrix  $\mathbf{S}$  such that  $\mathbf{D} = \mathbf{S}^{-1} \mathbf{C} \mathbf{S}$ . By virtue of [75, Corollary 1.3.4], similar matrices have the same eigenvalues. Since  $\mathbf{L}^{-1} \mathbf{A} \mathbf{L}^{-H}$  and  $(\mathbf{L}\mathbf{L}^H)^{-1} \mathbf{A}$  are similar with similarity matrix  $\mathbf{L}^H$ ,  $\lambda_{\max}(\mathbf{L}^{-1} \mathbf{A} \mathbf{L}^{-H}) = \lambda_{\max}(\mathbf{B}^{-1} \mathbf{A}) = \lambda_{\max}(\mathbf{A}, \mathbf{B})$ .

Let  $\tilde{\mathbf{y}}$  be an eigenvector of  $\mathbf{L}^{-1} \mathbf{A} \mathbf{L}^{-H}$  corresponding to the maximum eigenvalue  $\lambda_{\max}$ . Then, by [75, Definition 1.1.2],  $\mathbf{L}^{-1} \mathbf{A} \mathbf{L}^{-H} \tilde{\mathbf{y}} = \lambda_{\max} \tilde{\mathbf{y}}$ . Multiplying both sides from the left by  $\tilde{\mathbf{y}}^H$  and substituting  $\tilde{\mathbf{y}} = \mathbf{L}^H \tilde{\mathbf{x}}$ , we obtain

$$\begin{aligned} (\mathbf{L}^H \tilde{\mathbf{x}})^H \mathbf{L}^{-1} \mathbf{A} \mathbf{L}^{-H} (\mathbf{L}^H \tilde{\mathbf{x}}) &= \lambda_{\max} (\mathbf{L}^H \tilde{\mathbf{x}})^H (\mathbf{L}^H \tilde{\mathbf{x}}) \\ \Leftrightarrow \tilde{\mathbf{x}}^H \mathbf{A} \tilde{\mathbf{x}} &= \lambda_{\max} \tilde{\mathbf{x}}^H \mathbf{B} \tilde{\mathbf{x}}. \end{aligned} \quad (76)$$

This establishes that  $\mathbf{L}^H \tilde{\mathbf{x}}$  maximizes  $\mathbf{x}^H \mathbf{A} \mathbf{x} / (\mathbf{x}^H \mathbf{B} \mathbf{x})$ . Due to similarity and the fact that  $\tilde{\mathbf{y}}$  is an eigenvector of  $\mathbf{L}^{-1} \mathbf{A} \mathbf{L}^{-H}$  corresponding to  $\lambda_{\max}$ ,  $\tilde{\mathbf{x}}$  is an eigenvector of  $\mathbf{B}^{-1} \mathbf{A}$  [75, Th. 1.4.8]. ■

## APPENDIX C EXPLICIT FORMULA FOR $D_{S,\text{OPT}}$

For the sake of brevity, only the case  $\cos(\theta_\ell^{\text{el}}) \geq \cos(\theta_{\ell-1}^{\text{el}})$  is considered here. The formula for the other case can be found in the same way. With (69b) and (66),  $\vartheta_{\ell-1}^{\text{el}}$  can be written as a function of the elevation angle  $\theta_\ell^{\text{el}}$  of satellite  $\ell$  and the receive array parameters  $\nu d_{A} N_r^x$

$$\begin{aligned} \vartheta_{\ell-1}^{\text{el}} &= \arccos \left( \cos(\theta_\ell^{\text{el}}) - \frac{2\pi}{\nu d_{A} N_r^x} \right) \\ &\quad + \arcsin \left( \frac{r_E}{r_0} \left( \cos(\theta_\ell^{\text{el}}) - \frac{2\pi}{\nu d_{A} N_r^x} \right) \right). \end{aligned} \quad (77)$$

Now, with (67), the distances  $d_{\ell-1}$  and  $d_\ell$  can be written as a function of  $\theta_\ell^{\text{el}}$ , the receive array parameters  $\nu d_{A} N_r^x$  as well as the orbital radius  $r_0$

$$\begin{aligned}
D_{S,\text{opt}} = r_0^2 & \left[ \left( \frac{\cos\left(\theta_\ell^{\text{el}} + \arcsin\left(\frac{r_E}{r_0} \cos(\theta_\ell^{\text{el}})\right)\right)}{\cos(\theta_\ell^{\text{el}})} \right)^2 \right. \\
& + \left( \frac{\cos\left(\arccos\left(\cos(\theta_\ell^{\text{el}}) - \frac{2\pi}{vd_A N_r^{\text{w}}}\right) + \arcsin\left(\frac{r_E}{r_0} \left(\cos(\theta_\ell^{\text{el}}) - \frac{2\pi}{vd_A N_r^{\text{w}}}\right)\right)\right)}{\cos(\theta_\ell^{\text{el}}) - \frac{2\pi}{vd_A N_r^{\text{w}}}} \right)^2 \\
& - 2 \frac{\cos\left(\theta_\ell^{\text{el}} + \arcsin\left(\frac{r_E}{r_0} \cos(\theta_\ell^{\text{el}})\right)\right)}{\cos(\theta_\ell^{\text{el}})} \\
& \cdot \frac{\cos\left(\arccos\left(\cos(\theta_\ell^{\text{el}}) - \frac{2\pi}{vd_A N_r^{\text{w}}}\right) + \arcsin\left(\frac{r_E}{r_0} \left(\cos(\theta_\ell^{\text{el}}) - \frac{2\pi}{vd_A N_r^{\text{w}}}\right)\right)\right)}{\cos(\theta_\ell^{\text{el}}) - \frac{2\pi}{vd_A N_r^{\text{w}}}} \\
& \left. \cdot \cos\left(\arccos\left(\cos(\theta_\ell^{\text{el}}) - \frac{2\pi}{vd_A N_r^{\text{w}}}\right) - \theta_\ell^{\text{el}}\right) \right]^{\frac{1}{2}}. \quad (79)
\end{aligned}$$

$$\begin{aligned}
d_{\ell-1} = r_0 & \left[ \left( \cos\left(\arccos\left(\cos(\theta_\ell^{\text{el}}) - \frac{2\pi}{vd_A N_r^{\text{x}}}\right) \right. \right. \\
& \left. \left. + \arcsin\left(\frac{r_E}{r_0} \left(\cos(\theta_\ell^{\text{el}}) - \frac{2\pi}{vd_A N_r^{\text{x}}}\right)\right)\right) \right) \\
& \cdot \left( \cos(\theta_\ell^{\text{el}}) - \frac{2\pi}{vd_A N_r^{\text{x}}} \right)^{-1} \Big] \quad (78a)
\end{aligned}$$

$$d_\ell = r_0 \frac{\cos\left(\theta_\ell^{\text{el}} + \arcsin\left(\frac{r_E}{r_0} \cos(\theta_\ell^{\text{el}})\right)\right)}{\cos(\theta_\ell^{\text{el}})}. \quad (78b)$$

Finally, plugging (78) into (68) gives the smallest optimal inter-satellite distance  $D_{S,\text{opt}}$

## REFERENCES

- [1] M. Röper, B. Matthiesen, D. Wübben, P. Popovski, and A. Dekorsy, "Beamspace MIMO for satellite swarms," in *Proc. IEEE Wireless Commun. Netw. Conf. (WCNC)*, Austin, TX, USA, 2022, pp. 1307–1312.
- [2] M. Röper, B. Matthiesen, D. Wübben, P. Popovski, and A. Dekorsy, "Robust precoding via characteristic functions for VSAT to multi-satellite uplink transmission," in *Proc. IEEE Int. Conf. Commun. (ICC)*, Rome, Italy, 2023, pp. 6281–6286.
- [3] "Study on using satellite access in 5G; (Release 16), Version 16.0.0," 3GPP, Sophia Antipolis, France, Rep. TR 22.822, Jun. 2018.
- [4] O. Kodheli et al., "Satellite communications in the new space era: A survey and future challenges," *IEEE Commun. Surveys Tuts.*, vol. 23, no. 1, pp. 70–109, 1st Quart., 2021.
- [5] I. del Portillo, B. G. Cameron, and E. F. Crawley, "A technical comparison of three low earth orbit satellite constellation systems to provide global broadband," *Acta Astronaut.*, vol. 159, pp. 123–135, Jun. 2019.
- [6] B. Di, L. Song, Y. Li, and H. V. Poor, "Ultra-dense LEO: Integration of satellite access networks into 5G and beyond," *IEEE Trans. Wireless Commun.*, vol. 26, no. 2, pp. 62–69, Apr. 2019.
- [7] I. Leyva-Mayorga et al., "LEO small-satellite constellations for 5G and beyond-5G communications," *IEEE Access*, vol. 8, pp. 184955–184964, 2020.
- [8] D. Tse and P. Viswanath, *Fundamentals of Wireless Communication*. Cambridge, U.K.: Cambridge Univ. Press, 2005.
- [9] R. T. Schwarz, T. Delamotte, K.-U. Storek, and A. Knopp, "MIMO applications for multibeam satellites," *IEEE Trans. Broadcast.*, vol. 65, no. 4, pp. 664–681, Dec. 2019.
- [10] L. You, K.-X. Li, J. Wang, X. Gao, X.-G. Xia, and B. Ottersten, "Massive MIMO transmission for LEO satellite communications," *IEEE J. Sel. Areas Commun.*, vol. 38, no. 8, pp. 1851–1865, Aug. 2020.
- [11] K. Storek, C. A. Hofmann, and A. Knopp, "Measurements of phase fluctuations for reliable MIMO space communications," in *Proc. IEEE Asia-Pac. Conf. Wireless Mob. (APWiMob)*, Bandung, Indonesia, 2015, pp. 157–162.
- [12] F. Yamashita, K. Kobayashi, M. Ueba, and M. Umehira, "Broadband multiple satellite MIMO system," in *Proc. IEEE Veh. Tech. Conf. (VTC)*, Dallas, TX, USA, 2005, pp. 2632–2636.
- [13] K. Liolis, A. Panagopoulos, and P. Cottis, "Multi-satellite MIMO communications at Ku-band and above: Investigations on spatial multiplexing for capacity improvement and selection diversity for interference mitigation," *EURASIP J. Wireless Commun. Netw.*, vol. 2007, Dec. 2007, Art. no. 59608.
- [14] D. Goto, H. Shibayama, F. Yamashita, and T. Yamazato, "LEO-MIMO satellite systems for high capacity transmission," in *Proc. IEEE Glob. Commun. Conf. (GLOBECOM)*, Abu Dhabi, UAE, 2018, pp. 1–6.
- [15] M. Caus, M. Shaat, A. I. Pérez-Neira, M. Schellmann, and H. Cao, "Reliability oriented OTFS-based LEO satellites joint transmission scheme," in *Proc. IEEE Globecom Workshops (GC Wkshps)*, 2022, pp. 1406–1412.
- [16] S. Buzzi et al., "LEO satellite diversity in 6G non-terrestrial networks: OFDM vs. OTFS," *IEEE Commun. Lett.*, vol. 27, no. 11, pp. 3013–3017, Nov. 2023.
- [17] C. J. M. Verhoeven, M. J. Bentum, G. L. E. Monna, J. Rotteveel, and J. Guo, "On the origin of satellite swarms," *Acta Astronaut.*, vol. 68, nos. 7–8, pp. 1392–1395, Apr./May 2011.
- [18] G. Bacci, R. D. Gaudenzi, M. Luise, L. Sanguinetti, and E. Sebastiani, "Formation-of-arrays antenna technology for high-throughput mobile nonterrestrial networks," *IEEE Trans. Aerosp. Electron. Syst.*, vol. 59, no. 5, pp. 4919–4935, Oct. 2023.
- [19] D. Tuzi, T. Delamotte, and A. Knopp, "Satellite swarm-based antenna arrays for 6G direct-to-cell connectivity," *IEEE Access*, vol. 11, pp. 36907–36928, 2023.
- [20] D. Tuzi, T. Delamotte, M. Röper, A. Schröder, B. Matthiesen, and A. Knopp, "Multi-beam analysis of satellite swarm-based antenna arrays for 6G direct-to-cell connectivity," in *Proc. IEEE Future Netw. World Forum (FNWF)*, Baltimore, MD, USA, 2023, pp. 1–6.
- [21] R. Radhakrishnan, W. W. Edmonson, F. Afghah, R. M. Rodriguez-Osorio, F. Pinto, and S. C. Burleigh, "Survey of inter-satellite communication for small satellite systems: Physical layer to network layer view," *IEEE Commun. Surveys Tuts.*, vol. 18, no. 4, pp. 2442–2473, 4th Quart., 2016.
- [22] G.-P. Liu and S. Zhang, "A survey on formation control of small satellites," *Proc. IEEE*, vol. 106, no. 3, pp. 440–457, Mar. 2018.

- [23] H. Sampath, P. Stoica, and A. Paulraj, "Generalized linear precoder and decoder design for MIMO channels using the weighted MMSE criterion," *IEEE Trans. Commun.*, vol. 49, no. 12, pp. 2198–2206, Dec. 2001.
- [24] A. Wiesel, Y. C. Eldar, and S. Shamai, "Linear precoding via conic optimization for fixed MIMO receivers," *IEEE Trans. Signal Process.*, vol. 54, no. 1, pp. 161–176, Jan. 2006.
- [25] W. Yu and T. Lan, "Transmitter optimization for the multi-antenna downlink with per-antenna power constraints," *IEEE Trans. Signal Process.*, vol. 55, no. 6, pp. 2646–2660, Jun. 2007.
- [26] G. Zheng, S. Chatzinotas, and B. Ottersten, "Generic optimization of linear precoding in multibeam satellite systems," *IEEE Trans. Wireless Commun.*, vol. 11, no. 6, pp. 4695–4707, Jun. 2012.
- [27] V. Joroughi, M. Á. Vázquez, and A. I. Pérez-Neira, "Precoding in multigateway multibeam satellite systems," *IEEE Trans. Wireless Commun.*, vol. 15, no. 7, pp. 4944–4956, Jul. 2016.
- [28] A. I. Perez-Neira, M. A. Vazquez, M. B. Shankar, S. Maleki, and S. Chatzinotas, "Signal processing for high-throughput satellites: Challenges in new interference-limited scenarios," *IEEE Signal Process. Mag.*, vol. 36, no. 4, pp. 112–131, Jul. 2019.
- [29] L. You et al., "Hybrid analog/digital precoding for downlink massive MIMO LEO satellite communications," *IEEE Trans. Wireless Commun.*, vol. 21, no. 8, pp. 5962–5976, Aug. 2022.
- [30] W. Guo, A.-A. Lu, X. Gao, and X.-G. Xia, "Broad coverage precoder design for synchronization in satellite massive MIMO systems," *IEEE Trans. Commun.*, vol. 69, no. 8, pp. 5531–5545, Aug. 2021.
- [31] K.-X. Li et al., "Downlink transmit design for massive MIMO LEO satellite communications," *IEEE Trans. Commun.*, vol. 70, no. 2, pp. 1014–1028, Feb. 2022.
- [32] A. Im, D. Kerr, H. Lu, S. Wu, Z. Aliyazicioglu, and H. K. Hwang, "Angle of arrival estimation using MIMO array antenna," in *Proc. MTS/IEEE Oceans*, Bergen, Norway, 2013, pp. 1–4.
- [33] H. Lin, F. Gao, S. Jin, and G. Y. Li, "A new view of multi-user hybrid massive MIMO: Non-orthogonal angle division multiple access," *IEEE J. Sel. Areas Commun.*, vol. 35, no. 10, pp. 2268–2280, Oct. 2017.
- [34] F. Dietrich, *Robust Signal Processing for Wireless Communications* (Foundations in Signal Processing, Communications and Networking). Berlin, Heidelberg, Germany: Springer, 2008.
- [35] A. Abrardo, G. Fodor, M. Moretti, and M. Telek, "MMSE receiver design and SINR calculation in MU-MIMO systems with imperfect CSI," *IEEE Wireless Commun. Lett.*, vol. 8, no. 1, pp. 269–272, Feb. 2019.
- [36] Y. Guo and B. Levy, "Robust MSE equalizer design for MIMO communication systems in the presence of model uncertainties," *IEEE Trans. Signal Process.*, vol. 54, no. 5, pp. 1840–1852, May 2006.
- [37] D. Mi, M. Dianati, L. Zhang, S. Muhaidat, and R. Tafazolli, "Massive MIMO performance with imperfect channel reciprocity and channel estimation error," *IEEE Trans. Commun.*, vol. 65, no. 9, pp. 3734–3749, Sep. 2017.
- [38] S. Bazzi and W. Xu, "Robust Bayesian precoding for mitigation of TDD hardware calibration errors," *IEEE Signal Process. Lett.*, vol. 23, no. 7, pp. 929–933, Jul. 2016.
- [39] L. Sun et al., "A robust secure hybrid analog and digital receive beamforming scheme for efficient interference reduction," *IEEE Access*, vol. 7, pp. 22227–22234, 2019.
- [40] B. Carlson, "Covariance matrix estimation errors and diagonal loading in adaptive arrays," *IEEE Trans. Aerosp. Electron. Syst.*, vol. 24, no. 4, pp. 397–401, Jul. 1988.
- [41] K. L. Bell, Y. Ephraim, and H. L. Van Trees, "A Bayesian approach to robust adaptive beamforming," *IEEE Trans. Signal Process.*, vol. 48, no. 2, pp. 386–398, Feb. 2000.
- [42] X. Mao, W. Li, Y. Li, Y. Sun, and Z. Zhai, "Robust adaptive beamforming against signal steering vector mismatch and jammer motion," *Int. J. Antennas Propag.*, vol. 2015, pp. 247–267, Jul. 2015.
- [43] Z. Li, Y. Zhang, Q. Ge, and B. Xue, "A robust deceptive jamming suppression method based on covariance matrix reconstruction with frequency diverse array MIMO radar," in *Proc. IEEE Int. Conf. Signal Process., Commun. Comput. (ICSPCC)*, Xiamen, China, 2017, pp. 1–5.
- [44] Z. Lin, M. Lin, B. Champagne, W. Zhu, and N. Al-Dhahir, "Robust hybrid beamforming for satellite-terrestrial integrated networks," in *Proc. IEEE Int. Conf. Acoust., Speech Signal Process. (ICASSP)*, Barcelona, Spain, 2020, pp. 8792–8796.
- [45] Y. Liu, Y. Wang, J. Wang, L. You, W. Wang, and X. Gao, "Robust downlink precoding for LEO satellite systems with per-antenna power constraints," *IEEE Trans. Veh. Technol.*, vol. 71, no. 10, pp. 10694–10711, Oct. 2022.
- [46] A. Schröder, S. Gracla, M. Röper, D. Wübben, C. Bockelmann, and A. Dekorsy, "Flexible robust beamforming for multibeam satellite downlink using reinforcement learning," in *Proc. IEEE Int. Conf. Commun. (ICC)*, Denver, CO, USA, 2024, pp. 3809–3814.
- [47] H. Joudeh and B. Clerckx, "Sum-rate maximization for linearly precoded downlink multiuser MISO systems with partial CSIT: A rate-splitting approach," *IEEE Trans. Commun.*, vol. 64, no. 11, pp. 4847–4861, Nov. 2016.
- [48] J. Lee, J. Lee, L. Yin, W. Shin, and B. Clerckx, "Coordinated rate-splitting multiple access for integrated satellite-terrestrial networks with super-common message," *IEEE Trans. Veh. Technol.*, vol. 73, no. 2, pp. 2989–2994, Feb. 2024.
- [49] A. Schröder, M. Röper, B. Matthiesen, D. Wübben, P. Popovski, and A. Dekorsy, "A comparison between RSMA, SDMA, and OMA in multibeam LEO satellite systems," in *Proc. Int. ITG 26th Workshop Smart Antennas 13th Conf. Syst., Commun., Coding*, Braunschweig, Germany, 2023, pp. 1–6.
- [50] A. Budianu, A. Meijerink, and M. Bentum, "Swarm-to-Earth communication in OLFAR," *Acta Astronaut.*, vol. 107, pp. 14–19, Feb./Mar. 2015.
- [51] M. Y. Abdelsadek, G. K. Kurt, and H. Yanikomeroglu, "Distributed massive MIMO for LEO satellite networks," *IEEE Open J. Commun. Soc.*, vol. 3, pp. 2162–2177, 2022.
- [52] S. Gracla, A. Schröder, M. Röper, C. Bockelmann, D. Wübben, and A. Dekorsy, "Learning model-free robust precoding for cooperative multibeam satellite communications," in *Proc. IEEE Int. Conf. Acoustics, Speech Signal Process. (ICASSP)*, Rhodes, Greece, 2023, pp. 1–5.
- [53] R. Richter, I. Bergel, Y. Noam, and E. Zehavi, "Downlink cooperative MIMO in LEO satellites," *IEEE Access*, vol. 8, pp. 213866–213881, 2020.
- [54] H. Kobayashi, B. L. Mark, and W. Turin, *Probability, Random Processes, and Statistical Analysis: Applications to Communications, Signal Processing, Queueing Theory and Mathematical Finance*. Cambridge, U.K.: Cambridge Univ. Press, 2011.
- [55] "Study on new radio (NR) to support non-terrestrial networks; (Release 15), Version 15.2.0," 3GPP, Sophia Antipolis, France, Rep. TR 38.811, Sep. 2019.
- [56] *Attenuation by Atmospheric Gases and Related Effects*, ITU-Rec. P. 676-12, Int. Telecommun. Union, Geneva, Switzerland, Aug. 2019.
- [57] *Propagation Data and Prediction Method Required for the Design of Earth-Space Telecommunication System*, ITU-Rec. P. 618-13, Int. Telecommun. Union, Geneva, Switzerland, Dec. 2017.
- [58] *Inospheric Propagation Data and Prediction Methods Required for the Design of Satellite Networks and Systems*, ITU-Rec P. 531-14, Int. Telecommun. Union, Geneva, Switzerland, Aug. 2019.
- [59] E. Telatar, "Capacity of multi-antenna Gaussian channels," *Eur. Trans. Telecommun.*, vol. 10, no. 6, pp. 585–595, Nov./Dec. 1999.
- [60] W. Wang, Y. Tong, L. Li, A.-A. Lu, L. You, and X. Gao, "Near optimal timing and frequency offset estimation for 5G integrated LEO satellite communication system," *IEEE Access*, vol. 7, pp. 113298–113310, 2019.
- [61] R. Rogalin et al., "Scalable synchronization and reciprocity calibration for distributed multiuser MIMO," *IEEE Trans. Wireless Commun.*, vol. 13, no. 4, pp. 1815–1831, Apr. 2014.
- [62] E. G. Larsson and J. Vieira, "Phase calibration of distributed antenna arrays," *IEEE Commun. Lett.*, vol. 27, no. 6, pp. 1619–1623, Jun. 2023.
- [63] M. M. Rahman, S. Dasgupta, and R. Mudumbai, "A distributed consensus approach to synchronization of RF signals," in *Proc. IEEE Stat. Signal Process. Workshop (SSP)*, 2012, pp. 281–284.
- [64] K. Yamamoto, C. Vorndamme, O. Hartwig, M. Staab, T. S. Schwarze, and G. Heinzel, "Experimental verification of intersatellite clock synchronization at LISA performance levels," *Phys. Rev. D*, vol. 105, Feb. 2022, Art. no. 42009. [Online]. Available: <https://link.aps.org/doi/10.1103/PhysRevD.105.042009>
- [65] "18th space defense squadron (18 SDS)." Space-track. Accessed: Sep. 7, 2024. [Online]. Available: <https://www.space-track.org>

- [66] T. Kelso. "CelesTrak." Accessed: Sep. 7, 2024. [Online]. Available: <http://celestrak.org/>
- [67] F. R. Hoots and R. L. Roehrich, "Models for propagation of NORAD element sets, project space track," Aerosp. Defense Command, Colorado Springs, CO, USA, Rep. 3, Dec. 1980.
- [68] D. A. Vallado, P. Crawford, R. Hujsak, and T. S. Kelso, "Revisiting spacetrack report #3: Rev 3," Am. Inst. Aeronaut. Astronaut., Reston, VA, USA, Rep. AIAA 2006-6753, 2007.
- [69] L. Pan et al., "Satellite availability and point positioning accuracy evaluation on a global scale for integration of GPS, GLONASS, BeiDou and Galileo," *Adv. Space Res.*, vol. 63, no. 9, pp. 2696–2710, 2017.
- [70] D. Brasoveanu, J. Hashmall, and D. Baker, "Spacecraft attitude determination accuracy from mission experience," Nat. Aeronaut. Space Admin., Washington, DC, USA, Rep. TM 104613, Oct. 1994.
- [71] T. Yoshioka and M. Murata, "An assessment of GPS-based precise point positioning of the low earth-orbiting satellite CHAMP," in *Proc. ICCAS-SICE*, Kukuoka, Japan, 2009, pp. 4722–4728.
- [72] D. P. Bertsekas, *Nonlinear Programming* (Athena Scientific Optimization and Computation Series), 2nd ed. Belmont, MA, USA: Athena Sci., 1999.
- [73] P. Patcharamaneepakorn, S. Armour, and A. Doufexi, "On the equivalence between SLNR and MMSE precoding schemes with single-antenna receivers," *IEEE Commun. Lett.*, vol. 16, no. 7, pp. 1034–1037, Jul. 2012.
- [74] E. A. Jorswieck and H. Boche, *Majorization and Matrix Monotone Functions in Wireless Communications*, vol. 3. Boston, MA, USA: Now Publ., 2007.
- [75] R. A. Horn and C. R. Johnson, *Matrix Analysis*. Cambridge, U.K.: Cambridge Univ. Press, 1990.
- [76] "Solutions for NR to support non-terrestrial networks (NTN); (Release 16), Version 16.0.0," 3GPP, Sophia Antipolis, France, Rep. TR 38.821, Dec. 2019.
- [77] D. Dodds and M. Moher, "Spread spectrum synchronization for a LEO personal communications satellite system," in *Proc. Can. Conf. Electr. Comput. Eng.*, 1995, pp. 20–23.